

IMAGE-BASED WEIGHTED MEASURES OF SKELETAL STIFFNESS: CASE  
STUDIES OF GREAT APE MANDIBLES

By

N. B. BHATAVADEKAR

A THESIS PRESENTED TO THE GRADUATE SCHOOL  
OF THE UNIVERSITY OF FLORIDA IN PARTIAL FULFILLMENT  
OF THE REQUIREMENTS FOR THE DEGREE OF  
MASTER OF SCIENCE

UNIVERSITY OF FLORIDA

2004

Copyright 2003

by

N.B.Bhatavadekar

This thesis is dedicated to my parents.

## ACKNOWLEDGMENTS

The August of 2002 will always be a milestone for me, which is when I started graduate education at the University of Florida. I had come to UF with many expectations and hopes. Right at the onset, I had the good fortune of being accepted in two research groups, the Applied Biomechanics Lab, headed by Dr. Andrew Rapoff and the Dental Biomaterials Lab, chaired by Dr. Kenneth Anusavice.

It has been a fantastic learning experience at UF, not just in terms of academic knowledge, but also in terms of an overall exposure into various fascinating fields, and these two years have contributed immensely to my development as a person, and established a great foundation for further study.

I am indebted to Dr. Rapoff for his support and guidance over the last two years. I did not have a traditional engineering background, and he has truly been patient with a dentist (no pun intended!). Dr. Anusavice, whom I consider an icon in the field of dentistry, has provided me with not just inspiration, but also support and sage advice. During the course of this thesis, Dr. David Daegling has gone out of his way in helping me at crucial stages of the research. Dr. Edward Walsh has been a crucial member of my supervisory committee, and I am thankful to him for his help.

I could not have concentrated on my work here at UF without the support of my parents and relatives. They have been my greatest source of inspiration. I would also like to make a special mention of my friends Dave Pinto, Quentin, Jeff Leismer, Sameer,

Wes, Ruxi, Susan and Barbara who have all been instrumental in helping me with my research, and I thank them all.

## TABLE OF CONTENTS

	<u>Page</u>
ACKNOWLEDGMENTS .....	iv
LIST OF TABLES .....	viii
LIST OF FIGURES .....	ix
ABSTRACT .....	xi
CHAPTER	
1 INTRODUCTION AND BACKGROUND .....	1
2 METHODS AND MATERIALS .....	4
CT Images of the Mandible .....	4
Development and Validation of Weighted Moment of Inertia Matlab code .....	5
Use of Matlab Code for Analysis of CT images.....	8
Background Transformation using ‘Image transform’ Matlab code .....	8
Removal of Tooth and Cancellous bone from the CT images “Tooth Removal code” .....	8
Calculation of Biomechanical Properties by “Weighted moment of inertia” program .....	10
Scaling of Images to Compensate for Difference in Jaw Lengths.....	11
Transformation of Moment of Inertia Axes.....	12
Statistical Analysis.....	13
3 RESULTS .....	14
4 DISCUSSION.....	20
Effect of Grayscale Power .....	24
Conclusion .....	26
APPENDIX	
A SAMPLE MATLAB CODES.....	28
B VALIDATION OF MATLAB CODE.....	43

C	IMAGE PROCESSING.....	48
D	BASIC ANATOMY OF THE MANDIBLE.....	53
E	ADDITIONAL RESULTS.....	55
	LIST OF REFERENCES.....	59
	BIOGRAPHICAL SKETCH.....	62

## LIST OF TABLES

<u>Table</u>	<u>page</u>
3-1: Comparison of unweighted and weighted moments of inertia. The first two columns show % difference, while the last column shows difference. ....	14
3-2: Effect of weighing the moment of inertia on the rank ordering within the group. 14 Gorilla molar sections were used in this case.9 out of 14 sections changed their rank order.3 pairs swapped ranks (B&D,F&G,L&M) while 1 triplet permuted ranks(IJK &JKI). The coefficient of rank correlation (Kendall's tau) between weighted and unweighted is 0.85 (P<0.01).....	15
3-3: ANOVA table for (weighted Iyy/wishboning arm <sup>4</sup> )*10 <sup>4</sup> values from premolar sections of Gorilla, Pongo and Pan. ....	17
3-4: ANOVA table for (weighted Iyy/wishboning arm <sup>4</sup> )*10 <sup>4</sup> values obtained from premolar sections for Gorilla, Pongo and Pan, analyzed further from values obtained in Table 3-2.....	17
3-5: Fisher's PLSD test for (weighted Iyy/wishboning arm <sup>4</sup> )*10 <sup>4</sup> for premolar sections.	18
3-6: ANOVA table for (weighted Iyy/wishboning arm <sup>4</sup> )*10 <sup>4</sup> for symphyseal sections. The weighted Iyy used was the value obtained after axis transformation to the true anatomic axis for the symphyseal section. ....	18
3-7: Fisher's PLSD for (weighted Iyy/wishboning arm <sup>4</sup> )*10 <sup>4</sup> for symphyseal sections. ...	18

## LIST OF FIGURES

<u>Figure</u>	<u>page</u>
2-1: The shaded area represents the cortical bone portion of an anteromedial cross section through an ape mandible. ....	6
2-2: Cross section after removal of tooth and cancellous bone. ....	10
3-1: Comparison between the new1 (transformed to weighted axes) unweighted and weighted Ixx and Iyy. ....	16
4-1: Plot of the grayscale power, p, versus the logarithm (to base 10) of Ixxp and Iyyp. p has been varied from 0.9 to 1.1. Note that a power of 1, as shown in the plot would correspond with the Ixxp and Iyyp values calculated and compared for all sections in this study. ....	26
B-1. Composite cross sectional figure with different grayscale values. ....	43
B-2: Modification of Figure 1. The top right quadrant has been given the same grayscale value as the background (black-0). ....	44
B-3. Figure B-2 showing position of centroid and angle after running it through the New Matlab code. ....	45
B-4. Figure B-3 showing position of centroid and angle after running it through the New Matlab code. ....	46
B-5: Example of the comparison of results obtained for two composite circles with hand calculation and with the new Matlab code. ....	47
C-1: CT image seen after converting it into a bitmap using Tomovision software. The section on the right is the one to be considered, while the one on the left is to be discarded. The sections can be seen placed in a water bath, when they were scanned. ....	48
C-2: Image C-1 seen after cropping. The section seen is the right section, and the left has been deleted. (Image has been magnified here for clarity). ....	50
C-3: Figure C-2 after background transformation using 'Image transform' Matlab code. (Image magnified here). ....	50

C-4: Figure C-3 after running it through the ‘Weighted moment of inertia’ program. The user has the option of defining an axes parallel to the original axes. If this option is chosen, the ‘user specified axes’ will be displayed on the image. In the image above, these axes are not shown, as they were not selected.....	51
D-1: Anatomical features in the human mandible. <a href="http://www.tpub.com/dental1/14274_files/image066.jpg">http://www.tpub.com/dental1/14274_files/image066.jpg</a> , last accessed: 01/18/04.	53
D-2: Example of a CT scan taken through the premolar plane in the human mandible. For illustrative purposes, the mandible shown is a human mandible, while the cross section is actually a premolar section through an ape mandible. (Source: <a href="http://s.clayton.edu/biology/BIOL1151L/lab05/skull_whole.htm">s.clayton.edu/biology/BIOL1151L/lab05/skull_whole.htm</a> , last accessed: 01/24/04) .....	54
E-1: Plot of premolar sections from Gorilla, Pongo and Pan. The unweighted Ixx values are after axes transformation to the weighted Ixx axes.....	55
E-2: Comparison of two plots of the Gorilla molar section demonstrating the change in rank ordering within the sample group before and after weighing the moments of inertia. In the legend, the filled symbols indicate male sections, while the open symbols indicate female sections. ....	56
E-3: Plot of the unweighted scaled Iyy versus the weighted scaled Iyy for the Pan symphyseal, premolar and molar sections.....	57
E-4: Comparison of variation in theta ( $\theta_p$ ) with change in the $p$ . Each gorilla molar section tested is represented by a different trend line. ....	58

Abstract of Thesis Presented to the Graduate School  
of the University of Florida in Partial Fulfillment of the  
Requirements for the Degree of Master of Science

IMAGE-BASED WEIGHTED MEASURES OF SKELETAL STIFFNESS: CASE  
STUDIES OF GREAT APE MANDIBLES

By

Neel Bhatavadekar

May 2004

Chair: Andrew Rapoff

Major Department: Biomedical Engineering

Traditional measures of structural stiffness in the primate skeleton do not consider heterogeneous material stiffness distribution. Given the fact of bone heterogeneity, it would be logical to assume that the use of traditional measures would lead to errors in estimating the stiffness for that cross-section. Measures of weighted stiffness can be developed by including heterogeneous grayscale variations evident in computed tomographic (CT) images. Since grayscale correlates with material stiffness, the distribution of bone quality and quantity is simultaneously considered. We developed custom software to calculate weighted and unweighted measures of bending resistance at three locations along the mandibular corpus from CT images from Gorilla, Pongo, and Pan. The traditional (unweighted) moment of inertia is modified by weighing each pixel by its grayscale value in our technique.

This technique throws new light on biomechanical analysis of ape bone cross-sections. Our weighted and unweighted moments differ by up to 20%. The differences

are not predictable; hence they cannot be calculated simply by using the unweighted moments. We also discovered that the rank ordering within the species sample changes if weighted moments are considered. Also, since weighing the moments is a technique that incorporates both geometry and material distribution, the results obtained without using weighted moments would not be a true representation of the biomechanical properties of those cross-sections. The use of weighted measures is a more robust comparative measure and would help answer some perplexing questions in anthropology unanswered to date with the use of the traditional moments of inertia.

Key words: computed tomography, bone density, Great Apes, moment of inertia, mandible, bending stiffness.

## CHAPTER 1 INTRODUCTION AND BACKGROUND

Traditionally, measures of structural stiffness in bones do not consider the heterogeneous material stiffness distribution. Errors associated with the measurement of structural stiffness are very probable, but have largely remained undocumented. The objective of this research study is to develop a technique for incorporating the material variation of bone into measures of skeletal stiffness.

The technology of computerized tomography (CT) is ideal for comparative biomechanical investigations (which need an incorporation of both geometry and material distribution) since it is a nondestructive technique that permits the examination of large comparative samples. The major technological breakthrough of CT is that plane structures, such as mandibular cross-sections, can be visualized without interference of structures on either side of the section (Hounsfield, 1973). The use of CT scans to measure biomechanical properties is preferred over external linear dimensions because simplifying assumptions about cross-sectional geometry and bone distribution are circumvented (Demes et al, 1984).

Moreover, CT visually displays relative density of bone in terms of grayscale; lighter regions of an image indicate higher mineral density. This permits a more precise assessment of biomechanical function, since accurate images of cortical bone contours may be obtained (Ruff and Leo, 1986).

Previous work by authors such as Daegling (1989) and Taylor (2002) on the mandibles of “Great Apes” have essentially considered the geometry of the bone, and not its material heterogeneity, when deriving its biomechanical properties.

Previous study of mandibular cross-sectional morphology in great apes indicates that the necessary assumptions of geometric regularity implied using external linear measures led to significant errors in calculation of biomechanical properties in these taxa. (Daegling, 1989). In his later work, Daegling (2001), used CT scan images from Great Apes and performed biomechanical analysis by digitizing the images. The cortical bone contours were traced and digitized, and biomechanical variables calculated using an algorithm developed by Nagurka and Hayes. (1980). Grayscale variance (representing material bone density) was not considered in the analysis.

Techniques such as photodensitometric methods (Fukunaga et al.1990) have been used to access the density of bone per cross section. This and other methods such as single photon absorptiometry and dual photon absorptiometry primarily track the change in bone mineral content. Their objective is not to provide an index that combines the distribution of bone mineral with the geometry of the cross section. Weiss et al. (1998) have used acoustic techniques in combination with geometric parameters such as principal moments of inertia, polar moment of inertia, and the biomechanical shape index for comparisons between cross sections of the femur. A pulse transmission ultrasonic technique (Schwartz-Dabney and Dechow, 2003) has been made use of for studying the variations in elastic properties across the mandible, and also attempted to find the relationship between these properties and mandibular function.

Mayhew (et al. 2004) has used density-weighted cross-section moments of inertia derived from pQCT images as a measure of structural analysis for cases of hip fracture (Mayhew, 2004). Making use of attenuation coefficients to represent the gray scale values, he concluded that biomechanical analysis of the distribution of bone within the femoral neck may offer a marked improvement in the ability to discriminate patients with an increased risk of fracture. The technique did not make use of CT scan images as a direct input, but this method relied on the use of pQCT, which is a more expensive technique than the CT scan. Corcoran et al (1994) made use of mass weighted moments of inertia and bone cross-sectional area to study the changes in bone cross-sectional area in postmenopausal women. Weighted moments of inertia incorporate geometry and material distribution, hence would be a better estimator of biomechanics and ultimately; function. To the best of our knowledge, the use of weighted moments of inertia for reasons of comparison across CT images has not been attempted before in anthropology.

Heterogeneous grayscale variations present in computerized tomograph (CT) images are used in this research study. Since grayscale correlates with material stiffness (Ciarelli et al. 2003), both the distribution of bone quality as well as quantity is considered. Customized software is used to calculate weighted and unweighted measures of bending resistance at three locations along the mandibular corpus from CT images obtained from Great Apes. The results obtained with the weighted measures are then analyzed and interpreted for possible relation between diet and mandibular stiffness.

## CHAPTER 2 METHODS AND MATERIALS

### **CT Images of the Mandible**

CT images of the mandible from different species of apes were obtained from a previous study, not related to the present research. The species represented were *Gorilla gorilla*, *Pan troglodytes* (Chimpanzee) and *Pongo pygmaeus* (Orangutans). These taxa have characteristic diets; both *Gorilla* and *Pongo* consume a harder diet (Doran et al. 2002, MacKinnon, 1974) than *Pan troglodytes*, which consumes a diet consisting primarily of fleshy fruits (Kuroda, 1992). The stiffness and strength of the mandibular sections of these three taxa would also enable us to establish a correlation (if any) between biomechanical properties and diet.

The sections from the symphyseal (S), premolar (P4) and molar (M2) regions were selected for the image analysis, as these regions best represented the three different sites that experienced variable loading during functional movements of the mandible (such as in mastication) [Appendix D].

A total of 90 images (30 each from symphyseal, premolar and molar regions from *Gorilla*, *Pan troglodytes* and *Pongo*) were used. The gender of the specimen that the section came from was known, as was the jaw length for all specimens. The CT scans were performed on a GE CT 9800 machine with the following parameters common for all images taken- tube voltage- 120 kV, tube current- 170 mA, scan time- 4 seconds, slice thickness- 1.5 mm, and pixel dimension was either 0.49 X 0.49 mm or 0.25 X 0.25 mm. The different pixel dimension were accounted for in all calculations. (Appendix C). For

all the CT images, the specimens had been oriented such that the X axis is parallel to the lower image border and the Y axis is parallel to the left image border. In all image processing techniques used, this orientation is accurately maintained.

All the CT images were taken using the same fixed orientation, and these images were obtained in the GE CT 9800 format. These images were subsequently converted into grayscale bitmap images. The grayscale variance (0-255) refers to the distribution of hard tissue (essentially, the varying density of hard tissue) within a given region. This distribution is of critical importance, as it will dictate the mechanical properties of the region in consideration. For example, a section of bone that is considered as a piece with uniform distribution of matter will behave differently mechanically as compared to a section of bone that has greater bone density towards one end than the other.

The grayscale value is related to the mineral density of the bone (Gotzen et al. 2003). As we incorporate the grayscale value in our work, we effectively account for the material property and distribution (for bone).

### **Development and Validation of Weighted Moment of Inertia Matlab Code**

Consider the mandibular cross section in Figure 2-1. The area can be viewed as being discretized into differential areas  $\Delta A_i$  of identical size. The differential areas will become pixels when the analysis is performed using computer image analysis software, such as in Matlab<sup>TM</sup>

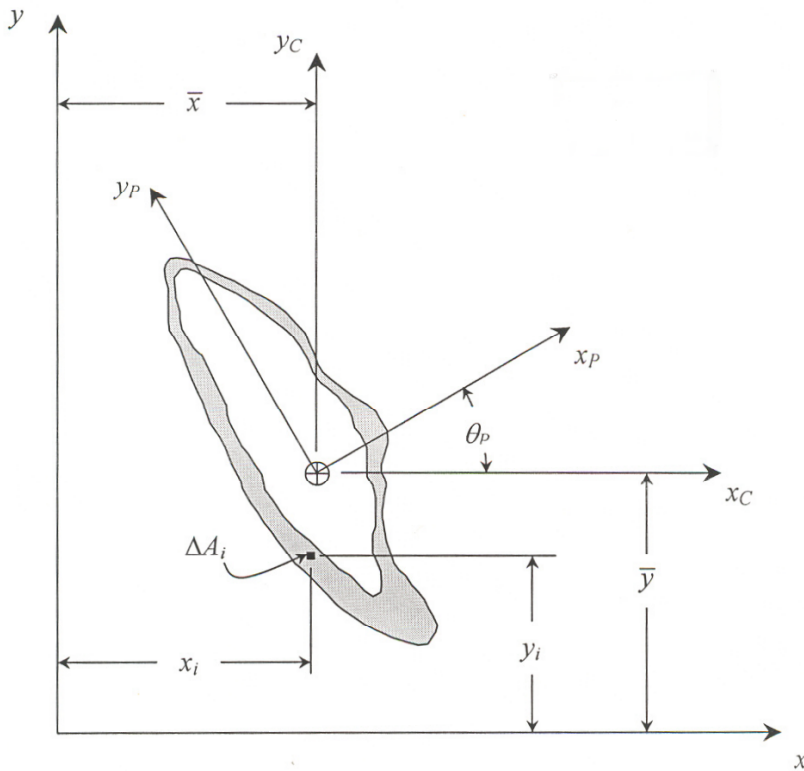


Figure 2-1: The shaded area represents the cortical bone portion of an anteromedial cross section through an ape mandible.

The area moments of inertia about the arbitrary axis x and y are

$$(I_{xx}, I_{yy}, I_{xy}) = (\sum y_i^2 \Delta A_i, \sum x_i^2 \Delta A_i, \sum x_i y_i \Delta A_i)$$

Since each pixel of area  $\Delta A_i$  has a grayscale value ( $\Gamma_i$ ), the above formula converts

to

$$(I_{xx}, I_{yy}, I_{xy}) = (\sum y_i^2 \Gamma_i \Delta A_i, \sum x_i^2 \Gamma_i \Delta A_i, \sum x_i y_i \Gamma_i \Delta A_i)$$

The distances of the centroidal axes  $x_c$  and  $y_c$  from the arbitrary axes x and y are

$$(\bar{x}, \bar{y}) = \left\{ \frac{\sum x_i \Gamma_i \Delta A_i}{\sum \Gamma_i \Delta A_i}, \frac{\sum y_i \Gamma_i \Delta A_i}{\sum \Gamma_i \Delta A_i} \right\}$$

Therefore, the weighted moments of inertia about the centroidal axes are

$$(I_{x_c x_c}, I_{y_c y_c}, I_{x_c y_c}) = \left( I_{xx} - \bar{y}^2 \sum \Gamma_i A_i, I_{yy} - \bar{x}^2 \sum \Gamma_i A_i, I_{xy} - \bar{x} \bar{y} \sum \Gamma_i A_i \right)$$

Thus, principal moments of inertia are

$$(I_{x_p p}, I_{y_p p}, I_{x_p y_p}) = \left( \frac{I_{x_c x_c} + I_{y_c y_c}}{2} + \sqrt{\left( \frac{I_{x_c x_c} - I_{y_c y_c}}{2} \right)^2 + I_{x_c y_c}^2}, \frac{I_{x_c x_c} + I_{y_c y_c}}{2} - \sqrt{\left( \frac{I_{x_c x_c} - I_{y_c y_c}}{2} \right)^2 + I_{x_c y_c}^2}, 0 \right)$$

The orientation  $\Theta_p$  of the principal axes with respect to the centroidal axes  $x_c$  is

$$\Theta_p = \frac{1}{2} \tan^{-1} \left[ \frac{2I_{x_c y_c}}{I_{x_c x_c} - I_{y_c y_c}} \right]$$

We established a Matlab<sup>TM</sup> image analysis program that took into account the individual grayscale value of each pixel (0-255) and calculated the centroid, principal moments ( $I_{xx}$ ,  $I_{yy}$ ), and the orientation ( $\Theta$ ) of the principal axes with respect to centroidal axes. All the pixels in the image, including the pixels constituting the background are included in the analysis. The cross-sectional image consists of pixels with differing grayscale values. Typically, the cortical bone appears denser (whiter in the CT image). Hence, it exhibits higher grayscale value than the cancellous bone. The grayscale value is a function of the mineral content of the area under consideration. Thus, the area of cortical bone representing a higher grayscale value than the less dense bone (with a lower grayscale value) contributed differently to the biomechanical property of the cross-section; and this was taken into account in the software program.

To validate the Matlab code, composite cross-sectional figures (such as composite circles, rectangles and triangles) with known grayscale values were examined. The hand-calculated results were compared with the results obtained through the New Matlab code. Both the results tallied for all figures, thereby validating the Matlab code. (Appendix b)

### **Use of Matlab Code for Analysis of CT images**

Tomovision™ 1.2 Rev-14 software was used for opening the GE CT9800 images and converting them into 8-bit bitmap images. This converts the data into an image format that can be analyzed with Matlab.

#### **Background Transformation using “Image transform” Matlab Code**

Some of the mandibular cross-sections had been scanned in a water bath, and some in air. This resulted in the background having a variable grayscale value. If this image was analyzed in this manner, the background grayscale value would have contributed to the moment of inertia, and it would have yielded erroneous results. To avoid this, it was necessary to ensure that the background for all the images had a uniform grayscale value of 0. For this purpose, a program was developed that transformed the background of all the bitmap images to a grayscale value of zero.

The bitmap image thus obtained has a background that represents a grayscale value of zero, and the cross-section of the mandible representing variable grayscale values, ranging from 0 to 255.

#### **Removal of Tooth and Cancellous Bone from the CT Images “Tooth removal Code”**

The CT image obtained after cropping shows the cross section through the mandible. This cross section includes the tooth and the cortical and cancellous bone forming the mandible. All three structures can be distinctly differentiated anatomically, and by the difference in the grayscale. For example, the tooth can be delineated from the rest of the cortical/cancellous bone simply by outlining the periodontal ligament space. In certain areas where the space may not be distinct, elementary anatomical knowledge of the root form assists the observer in demarcating the root form from the rest of the mandible.

In normal function, the masticatory loads are simply transferred by the teeth to the underlying bone. Here, it is important to understand the anatomy of the tooth-bone junction. The tooth is not fused to the supporting bone, but in fact, it is stabilized in the tooth socket by the periodontal ligament. This is a very thin membrane, about 0.5 mm in width, which serves to support the tooth in the socket, in addition to other functions such as nutrition and proprioception. During mastication, the tooth depresses slightly in the socket, compressing the periodontal ligament, and transferring the loads to the underlying bone. We assume that the tooth itself plays no part in contributing to the bending resistance of the jaw. The cancellous bone is located inferior to the cortical bone, and in the CT image, it can be seen as a honey-combed structure towards the center of the cross-section. This part contains only a few trabeculae, and bone marrow. Consideration of material property differences between compact and cancellous bone, suggests that even significant proportions of cancellous bone (10-40% of total cross-sectional area) will very likely have negligible effects on bone strength and rigidity, and can be effectively ignored in analyses of diaphyseal sections. (Ruff et al.1983).Daegling et al. (1992) demonstrated that for corpus twisting, the mandible, after removal of teeth, does not behave as a member with open or closed sections as predicted by theoretical models. Thus, we have assumed that the bending or torsional resistance by the mandible to stresses is chiefly a function of the cortical bone, with a very insignificant (or no) contribution from the tooth and /or cancellous portion of the bone. For this reason, we have chosen to not consider the tooth and the cancellous bone in the image analysis and subsequent calculations.

The CT images would thus have to be modified to exclude both the tooth and the cancellous bone. If the teeth were included in the final image analysis, they would

contribute to the weighted moment of inertia, and hence provide erroneous results, that could not be interpreted as a true representation of the mandibular resistance to stresses. The removal of the tooth and the cancellous portion of bone were accomplished by developing a 'Tooth removal' Matlab program, which allowed the user to manually select the area on the image to be removed

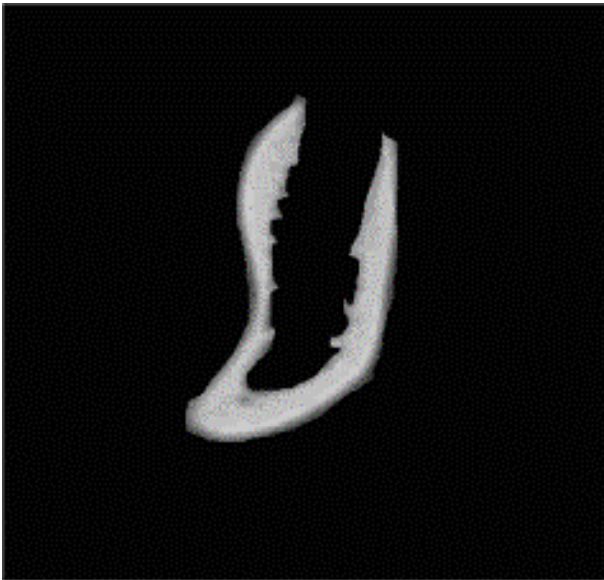


Figure 2-2: Cross section after removal of tooth and cancellous bone.

### **Calculation of biomechanical properties by 'Weighted moment of inertia' program**

The image is now suitable for analysis with the 'Weighted moment of inertia' Matlab code. Since the grayscale variation within the image has been preserved, the biomechanical properties will be a true reflection of the bone material as well as the geometry.

The X and Y axes are defined as being parallel to the bottom and left borders of the image respectively. The intra-observer error in removal of the tooth and cancellous bone from the rest of the cross-section was checked, with reference to the resultant change in angle theta ( $\Theta$ ). Ten images were selected randomly from the given pool of

images, and the tooth and cancellous bone was removed from each image three different times. The resultant images were analyzed with the ‘Weighted moment of inertia’ software program, and an error of +/- 0.03 degrees (theta) was noted.

The images were then analyzed using a Matlab code that was binary.i.e. it measured all grayscale values as either 0 (black) or 1 (white).[Appendix A]Using the same criteria as for the weighted analysis, the moments of inertia were obtained. These were referred to as the “Unweighted moment of inertia (Ixx and Iyy).”

### **Scaling of Images to Compensate for Difference in Jaw Lengths.**

Since the images are from different genera of apes, they demonstrate different sizes and shapes. For example, the Gorilla jaw length is the largest in the group. Thus, it is imperative that the moments of inertia recorded be corrected appropriately for the effect of jaw length, and a relative comparison of the ‘robusticity’ of the different jaws be achieved(Daegling,1992).

Moment arms may be used to assess how relatively resistant or ‘robust’ a given section is. In other words, longer moment arms require larger area moments to maintain stress levels at similar magnitude. (Daegling, 1992).Going by Hylander’s model (Hylander, 1979, 1988) of stress states in the mandible, the lengths of the moment arms used in a previous study (Daegling, 2001) were used for scaling purposes in this study. The moment arm for lateral transverse bending (wishboning) had been calculated (Daegling, 1992) as the distance from the posterior ramal border to the infradentale. (This translates into the total mandibular length).Hence, for each section (symphyseal, premolar or molar) the distance from the posterior ramal border to that section was used. The length of the moment arm in parasagittal bending had also been calculated by Daegling as the distance from infradentale to the plane of the CT section under

consideration. For the symphyseal section, the parasagittal moment arm length is zero. Thus, resistance to a mediolateral bending moment is calculated about vertical (Y-Y) axes.  $I_{xx}$  refers to resistance to parasagittal or vertical bending, while  $I_{yy}$  quantifies transverse bending rigidity.

We used the same ‘ $I_{xx}$ /Parasagittal moment arm’ and ‘ $I_{yy}$ /Wishboning moment arm’ ratio as used in the previous study by Daegling. The former describes the relative stiffness in parasagittal bending, while the latter ratio describes the relative stiffness in wishboning resistance. In order to provide dimensionless indices, fourth powers of the moment arms were used. (Daegling, 1992).

### **Transformation of Moment of inertia axes**

The “unweighted” and “weighted” moments of inertia for the same image differed in that they had different principal axes, given the fact that the weighted moment of inertia had been calculated taking into account the individual pixel grayscale values, which had not been done in the unweighted Matlab code. Hence, for the sake of comparison between the weighted and unweighted moments of inertia, it was necessary to transform the unweighted moments of inertia ( $I_{xx}$ ,  $I_{yy}$ ) to the weighted moment of inertia axes.

This was achieved using Mohr’s circle for transformation. The difference between the weighted and unweighted angle ( $\Theta$ ) was chosen as the angle for the Mohr’s transformation. The resultant values for the unweighted  $I_{xx}$  and  $I_{yy}$  (after axes transformation) could be compared with the weighted moments of inertia, as they were now about the same reference axes.

For the CT scanning, the premolar and molar sections had been oriented such that their anatomical axes corresponded very closely to the established principal axes.

However, the symphyseal sections were oriented such that their anatomical axis was almost at a 30-40 degree angle with the established principal axes. Hence, it was necessary to transform the unweighted and weighted  $I_{xx}$ ,  $I_{yy}$  to the same reference axes, as was done previously. The unweighted and weighted  $I_{xx}$ ,  $I_{yy}$  were transformed by their respective angles ( $\Theta$ ) to allow for a true comparison about the same axes.

### **Statistical Analysis**

We performed statistical analysis on the three taxa groups (Gorilla, Pongo and Pan) using Analysis of Variance (ANOVA) for each section (symphysis, premolar and molar). A SAS based software package (StatView<sup>TM</sup>) was used for all the statistical analyses.

Depending on the ANOVA results, select data groups were analyzed using Fisher's PLSD test. A p value of  $<0.05$  was considered to be significant.

### CHAPTER 3 RESULTS

The “weighted” and “unweighted” Matlab programs provided results for the  $I_{xx}$ ,  $I_{yy}$  and angle ( $\Theta$ ) for all 90 images. After appropriate axes transformation using Mohr’s transformation circle, (as previously described), the unweighted and weighted moments of inertia ( $I_{xx}$ ,  $I_{yy}$ ) could be compared. Table 3-1 enlists the percentage differences observed. For each taxon, the percentage difference between the unweighted and weighted  $I_{xx}$ ,  $I_{yy}$  was averaged over specific sections.

Table 3-1: Comparison of unweighted and weighted moments of inertia. The first two columns show % difference, while the last column shows difference.

Taxon	Section	% Difference between unweighted and weighted		Difference between unweighted and weighted $\Theta(^{\circ})$
		$I_{xx}$	$I_{yy}$	
Pongo	symphysis	12	11.9	0.13
	premolar	11.7	10.8	-0.90
	molar	21.6	21	-0.56
Gorilla	symphysis	14.8	15.4	-0.09
	premolar	15.6	14.7	-1.06
	molar	18.9	19.1	0.11
Pan	symphysis	18	19.7	-0.22
	premolar	17.5	16.8	0.21
	molar	20.1	19.6	-0.1

It can be observed from Table.1 that the difference between the unweighted and weighted moments of inertia ranges from 11.7 % for the Pongo premolar sections up to 21.6 % for the Pongo molar sections. (Lower value for weighted moment of inertia compared to unweighted).The values of  $I_{xx}$  and  $I_{yy}$  used were the “raw” values .i.e. prior to any axis transformation. All molar sections within each taxon demonstrate the most

difference in moment of inertia values (unweighted and weighted) compared to the premolar and symphyseal sections.

In order to investigate the effect of “weighing” the moment of inertia within the same taxon, and for the same section, we checked the rank ordering within the samples for that particular section. It was found that the rank ordering changes after weighing the moments of inertia.

Table 3-2: Effect of weighing the moment of inertia on the rank ordering within the group. 14 Gorilla molar sections were used in this case. 9 out of 14 sections changed their rank order. 3 pairs swapped ranks (B&D, F&G, L&M) while 1 triplet permuted ranks (IJK & JKI). The coefficient of rank correlation (Kendall’s tau) between weighted and unweighted is 0.85 ( $P < 0.01$ )

Rank	Unweighted Ixx	Weighted Ixx
1	A	A
2	B	D
3	C	C
4	D	B
5	E	E
6	F	G
7	G	F
8	H	H
9	I	J
10	J	K
11	K	I
12	L	M
13	M	L
14	N	N

Table 3-2 reveals that “weighing” the moment of inertia, in fact, changes the rank ordering within the group. We observed a similar change in rank ordering for other plots generated using symphyseal and premolar sections for all the three taxa. Since weighing of the moments of inertia appears to be a technique that would incorporate both geometry as well as material distribution, and since using this technique changes the rank ordering, this suggests that results obtained without using the weighted moments of inertia (using

just area moments of inertia, for example) would probably not be a true representation of the biomechanical properties for that cross section.

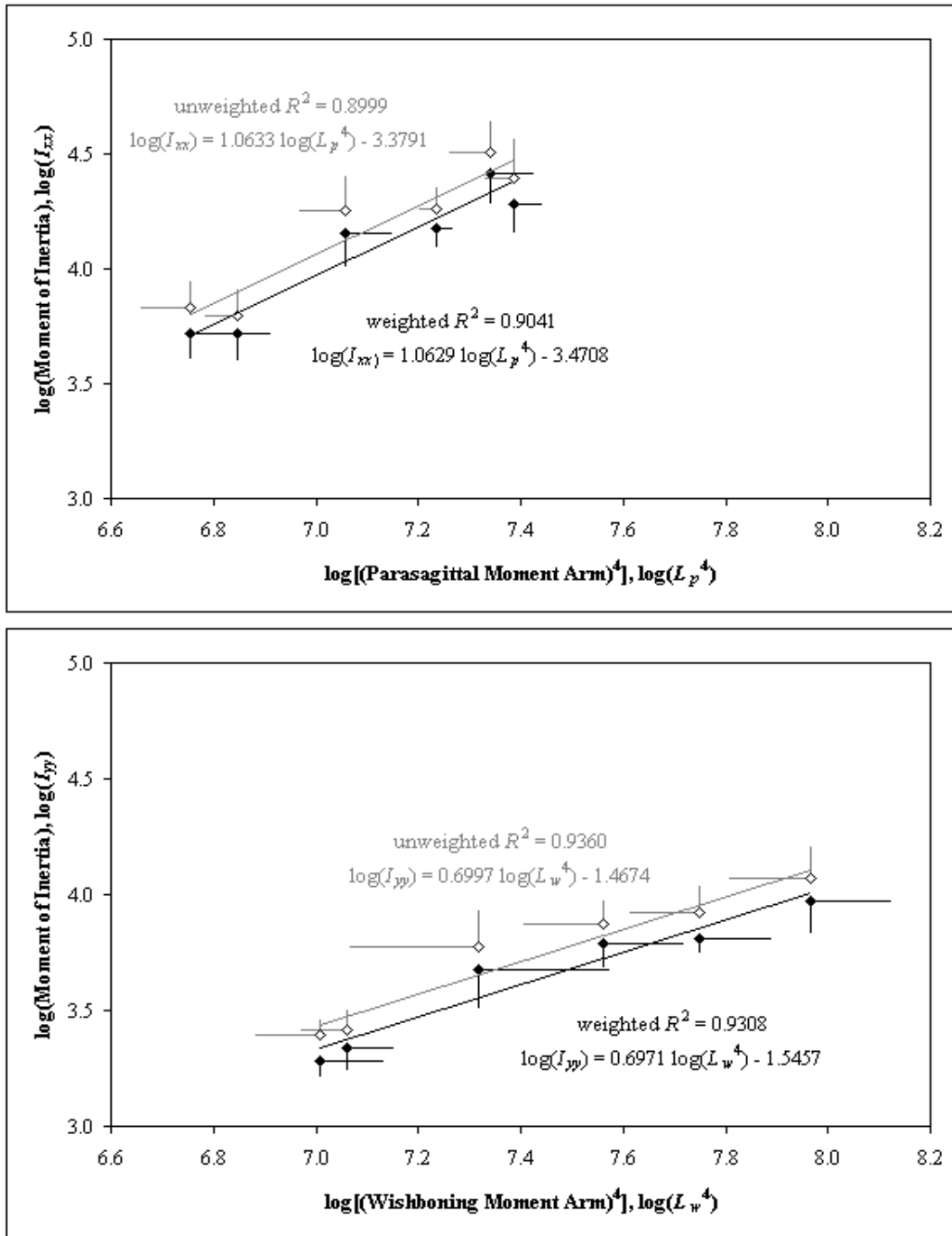


Figure 3-1: Comparison between the new1 (transformed to weighted axes) unweighted and weighted Ixx and Iyy.

<sup>1</sup>“New” refers to the unweighted Ixx and Iyy obtained after transforming the original axes to the weighted axes.

By averaging the values of Ixx (for each “new” unweighted and weighted Ixx) for male and female sections within each taxon, we obtained six points, (for three taxa) which were then used to plot a six point regression plot. Figure 3-1 shows this comparison .

### Statistical Analysis

To compare the Ixxp and Iyy across taxa, for a given section, we performed an Analysis of Variance (ANOVA) statistical test. We analyzed the weighted Ixx and Iyy values obtained for the molar, premolar and symphyseal sections of all taxa.

Table 3-3: ANOVA table for (weighted Iyy/wishboning arm<sup>4</sup>)\*10<sup>4</sup> values from premolar sections of Gorilla, Pongo and Pan.

Criteria	Degrees of Freedom	Sum of squares	Mean square	F-value	P-value	Lambda	Power
species	2	0.77	0.38	3.22	0.0576	6.44	0.55
sex	1	0.05	0.05	0.43	0.5204	0.43	0.09
species*sex	2	0.10	0.05	0.40	0.6744	0.80	0.11
Residual	24	2.85	0.12				

After removing effect of sex from above table, the results obtained are shown in

Table 3-4 below. A p-value<0.05 was considered as significant for all the analyses.

Table 3-4: ANOVA table for (weighted Iyy/wishboning arm<sup>4</sup>)\*10<sup>4</sup> values obtained from premolar sections for Gorilla, Pongo and Pan, analyzed further from values obtained in Table 3-2.

Criteria	Degrees of Freedom	Sum of squares	Mean square	F-value	P-value	Lambda	Power
species	2	0.96	0.48	4.29	<b>0.0241</b>	8.58	0.70
Residual	27	3.01	0.11				

Fisher’s PLSD analysis was performed for the effect of species from the values obtained from the ratio of (weighted Iyy/wishboning arm<sup>4</sup>)\*10<sup>4</sup>. (Table 3-4).

From Table 3-5, we observe that there is a statistically significant difference between Pan and Pongo (p=0.0257) and between Gorilla and Pongo (p=0.0099). This would indicate that for the premolar sections analyzed, the Gorilla molar section is less

stiff than the Pongo molar section. Also, that the Pan molar section is less stiff than the Pongo molar section.

Table 3-5: Fisher's PLSD test for (weighted Iyy/wishboning arm<sup>4</sup>)\*10<sup>4</sup> for premolar sections.

Criteria	Mean difference	Critical difference	P-value
Pan, Gorilla	0.03	0.30	0.8220
Pan, Pongo	-0.38	0.33	<b>0.0257</b>
Gorilla, Pongo	-0.42	0.31	<b>0.0099</b>

When we compared the weighted Ixx for molar sections for all three taxa, we found no statistically significant difference across the groups. Hence, one could conclude that even though the three taxa had different diets, there was no difference seen in the weighted Ixx values for the molar sections.

Table 3-6: ANOVA table for (weighted Iyy/wishboning arm<sup>4</sup>)\*10<sup>4</sup> for symphyseal sections. The weighted Iyy used was the value obtained after axis transformation to the true anatomic axis for the symphyseal section.

Criteria	Degree of Freedom	Sum of Squares	Mean square	F-value	P-value	Lambda	Power
species	2	0.59	0.29	3.54	0.0443	7.08	0.60
sex	1	8.35E-4	8.35E-4	0.01	0.9208	0.01	0.05
species*sex	2	0.09	0.05	0.55	0.5846	1.10	0.13
Residual	25	0.08					

Table 3-7: Fisher's PLSD for (weighted Iyy/wishboning arm<sup>4</sup>)\*10<sup>4</sup> for symphyseal sections.

Criteria	Mean difference	Critical difference	P-value
Pan, Gorilla	-0.31	0.25	<b>0.0164</b>
Pan, Pongo	-0.06	0.27	0.6647
Gorilla, Pongo	0.25	0.25	<b>0.0471</b>

We did not find a statistically significant difference between taxa for both weighted Ixx and weighted Iyy (scaled) in the molar sections. The Iyy obtained for the symphyseal sections after axis transformation to the true anatomical axis was subjected to an ANOVA test to check for difference across the three taxa. We found a statistically

significant difference between the symphyseal sections of Pan and Gorilla ( $p=0.0164$ ) and between symphyseal sections of Gorilla and Pongo ( $p=0.0471$ ). (Table 3-5, 3-6).

## CHAPTER 4 DISCUSSION

The image sections were all obtained from the (Great Apes) and from each of the following genus- Genus *Pongo*, Genus *Gorilla* and Genus *Pan*. These groups were of interest as they represented different dietary patterns. It was hence believed that a correlation between the biomechanical adaptation of the mandible and the dietary pattern could be made, based on the biomechanical properties calculated using the Matlab tool.

The diet of *Gorilla*, *Pan* and *Pongo* can be broadly described as being omnivorous. More specifically, western lowland gorillas (*Gorilla gorilla gorilla*) have been known to consume high quality herbs, bark, and a minimal diversity of fruits. Fibrous fruit species, such as *Duboscia macrocarpa* and *Klainedoxa gabonensis* were found to be an important dietary constituent. Also, no sex difference in diet has been detected. (Doran DM, 2002).

*Pongo* consumes a variety of hard unripe fruits, hard-husked objects such as seeds and bark, along with small amounts of insects, eggs and fungi. (MacKinnon, 1974, Ungar, 1995). *Pongo* subsists on a variety of hard food items which require large amounts of compressive, crushing components of the bite force. (Schwartz, 2000).

The *Pan troglodytes* diet is made up of about 70-80% fruit, 5-9 % seeds, 12-13.5% leaves, 3.5% pith and 3% flowers. (Kuroda, 1992, Tutin et al. 1997). *Pan* thus has a relatively softer diet than *Gorilla* and *Pongo*. *Gorilla*, *Pan* and *Pongo* can thus be divided into two categories- 1) Hard diet {*Gorilla*, *Pongo*} and 2) Soft diet {*Pan*}. Also, it would be interesting to note if the hard diet leads to an increased force for every bite, or increases the number of “bites” required. Hylander (1979) and Weijts and de Jongh (1977)

seem to indicate that a fibrous and hard diet leads to both increased force and increased cycles. Hence, it is postulated that harder diet would lead to increased stress on the underlying bone, causing it to remodel and make it stiffer, in order to resist the loading stresses.

We had hypothesized that due to the dietary difference in the two groups, Pan cross-sections would demonstrate markedly lower biomechanical stiffness, (reflected as lower principal moments of inertia about the X and Y axes, after adjusting for the respective jaw lengths), compared to the *Gorilla* and *Pongo* sections.

During unilateral mastication, the balancing side mandibular corpus is bent in a parasagittal plane so that the alveolar process is in tension while the base of the corpus is in compression. At the symphysis, the most important source of stress is created by lateral transverse bending, or “wishboning” of the mandibular corpora. Since wishboning bends the mandible in its plane of curvature, this bending moment causes the mandible to function as a curved beam. Daegling (1992) states that the optimal morphological solution for minimizing the effects of wishboning is to increase the labiolingual thickness of the symphysis. It is also quite possible that the optimal morphological solution might be to re-distribute the bone material which would produce more resistance, even with the same geometry.

We found up to a 20% difference between the unweighted and weighted  $I_{xx}$ ,  $I_{yy}$ . (Table 3-1) This difference was the maximum for molar sections within each taxon. The cortical bone for the molar sections appeared to be wider (thicker) than for the symphyseal and premolar sections for most CT sections. A larger cortical area would mean a greater grayscale variation. This would obviously be reflected as a greater

difference between the unweighted and weighted  $I_{xx}$  and  $I_{yy}$  as the cortical bone is considered to have uniform grayscale value of 255 for the unweighted calculations. If the difference between the unweighted and weighted moments of inertia was predictable, then this finding would not be very significant, as hypothetically, one could correct for this error in all future comparisons using the unweighted moments. However, since the rank ordering changes, the difference between the unweighted and weighted moment results is not predictable. In Figure 3-3 and 3-4, we observe that the slopes do not change dramatically, just the intercepts change for the linear regressions change as we weigh the moment of inertia. This seems to indicate that the plots do not scale allometrically across the taxa.

Taylor (2002) states that she had expected the *Gorilla* to show more compact bone in the corpus, and that it would demonstrate a deeper corpus, in keeping with the expected change in the mandibular stiffness due to the hard diet. She considered only the geometry (such as corpus depth), and not the material distribution. In essence, she used a solid beam model. Perhaps the analysis tool that we have used might be able to answer some of the discrepancies that she found between expected and observed results. It might be possible that the bone is redistributed in the *Gorilla* mandible, in response to the higher loads caused by harder diet, such that the stiffness increases without a significant increase in corpus depth.

We can observe that the *Gorilla* symphyseal section seems to have more resistance to wishboning stress than the *Pongo* symphyseal section. ( $p=0.0471$ ) (Table 3-6). However, we also can observe that the *Gorilla* premolar section appears to have lesser resistance to wishboning stress than the *Pongo* premolar section. ( $p= 0.0099$ )(Table 3-4).

Statistically, the results might appear to be conflicting, however, biologically, we know that the symphysis is often subjected to more stresses than the premolar section and molar section. (Hylander. 1979, 1984). Because of this, and because the symphysis acts like a curved beam, it is more important for the symphyseal section to resist bending stresses than the premolar sections. We hence feel that the result obtained for the symphyseal section is more relevant than the one for the premolar section. The  $I_{xx}$  and  $I_{yy}$  values for the molar sections showed no difference between taxa ( $p=0.2194$ ,  $p=0.1101$ ). Since the symphyseal sections routinely get more stresses than the molar section, it is quite probable that a difference in stiffness would be reflected more readily in the symphyseal region compared to the molar regions.

In the case of the symphyseal section, the weighted  $I_{yy}^1$  for the *Gorilla* is more than for *Pongo*. This could be interpreted as the biomechanical adaptation to a harder diet. In other words, this finding seems to be consistent with the diet of the *Gorilla*. For the molar sections, we did not find a significant difference for the scaled weighted  $I_{xx}$  and  $I_{yy}$  between the three taxa. We did find a difference between sexes for the molar (weighted and scaled)  $I_{yy}$  values. ( $p=0.0075$ ). Since the ramus of the mandible in the *Gorilla* and *Pongo* males is wider mesio-distally than for the females, the wishboning moment arm would obviously increase, which might lead to the difference observed. Since the male *Gorilla* jaws are the largest, if they do not proportionally widen as they increase in length, then the stress concentration would increase dramatically, keeping in mind a curved beam model.

---

<sup>1</sup> Refers to the value of  $I_{yy}$  obtained after transforming the axes to the true anatomical axes, and scaling appropriately using the (wishboning moment arm)<sup>4</sup> for dimensional consistency.

Previously, indices such as the robusticity index (ratio of corpus breadth to corpus height) (in Daegling, 1991), the ratio of  $I_{min}/I_{max}$  and  $I_{yy}/I_{xx}$ . (Daegling, 1992) have been used to provide an index of cross-sectional shape. However, it is important to note that these indices provide information solely about the shape of the cross section. We propose a new index: a ratio of “weighted  $I_{xx}$ /weighted  $I_{yy}$ ”, termed as a “consolidated index”. We believe that this would be a more robust ratio, as it incorporates both the geometry as well as the material distribution, compared to the ratios proposed by previous authors enlisted above which consider just the geometry.

### **Effect of Grayscale Power**

For cortical bone, radiographic grayscale is a power law function of apparent density  $\rho$ , over the range of physiologic apparent densities, or

$$\gamma = \alpha\rho^\beta + x$$

where  $\alpha$ ,  $\beta$  and  $x$  are constants. Solving for apparent density yields

$$\rho = \left( \frac{1}{\alpha} (\gamma - x) \right)^{1/\beta}$$

For cortical bone, modulus is a power law function of apparent density  $\rho$ , or

$$E = a\rho^b$$

where  $a$  is some constant, and the value of  $b=3.4$  (Currey, 1988). Substituting for apparent density yields

$$E = a \left( \frac{1}{\alpha} \gamma \right)^{b/\beta} = \frac{a}{\alpha^{b/\beta}} \gamma^{b/\beta}$$

Therefore, the modulus is proportional to grayscale to the power of  $b/\beta$ , or

$$E \propto \gamma^{b/\beta} = \gamma^p$$

In our weighted moment of inertia formulation, each pixel grayscale originally was raised to the power  $p = 1$ . In this way, the grayscale served as a direct surrogate for the modulus  $E$ . This would be true if the power  $\beta$  was around 3 as well.

Our unpublished laboratory data shows the value of  $\beta$  to be 3.8. Since  $b = 3.4$  (Currey, 1988), hence

$$\frac{b}{\beta} = 0.9, \text{ which is close to } 1.$$

The grayscale power  $p$  was varied from 0.9 to 1.1 to evaluate the effect on the weighted principal moments of inertia. The 14 gorilla molar sections were used in this analysis. When the logarithm of each moment (to base 10) is regressed against the grayscale power, the resulting regression lines have slopes and correlation coefficients as given in Figure 4-1.

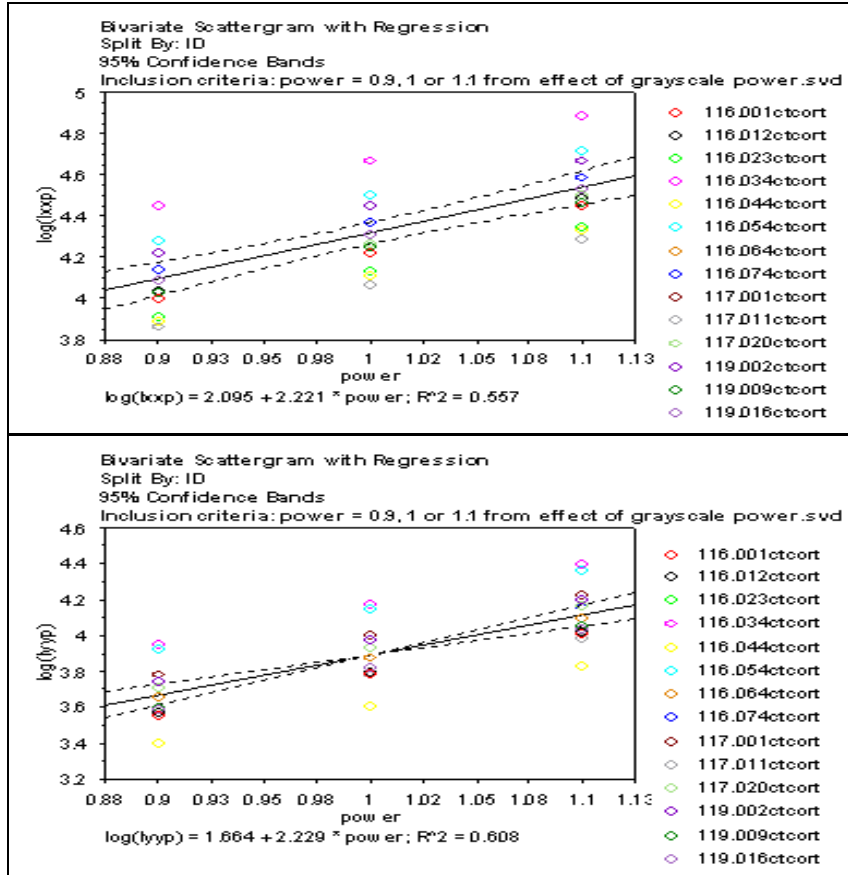


Figure 4-1: Plot of the grayscale power,  $p$ , versus the logarithm (to base 10) of  $I_{xxp}$  and  $I_{yyp}$ .  $p$  has been varied from 0.9 to 1.1. Note that a power of 1, as shown in the plot would correspond with the  $I_{xxp}$  and  $I_{yyp}$  values calculated and compared for all sections in this study.

The correlation coefficient ( $R^2$ ) is low (0.557, 0.608) (Figure 4-1) as the individual sections are very different from each other. The rank ordering within the group does not change when the grayscale power is changed. If a regression is run for three points (at grayscale values of 0.9, 1 and 1.1) of each section separately, we would get  $R^2=1$  for each of them. We could infer that grayscale power does have an effect on the absolute values of  $I_{xx}$ ,  $I_{yy}$  but does not have a large effect on the comparison of a sample group.

### Conclusion

We had hypothesized that the Pan sections would demonstrate relatively lower weighted moments of inertia than the Gorilla and Pongo sections, due to inherent

differences in diet, which would subject the mandibles to different loads across the taxa. We did not find a statistically significant difference between the taxa for all three sections; based on comparisons of the weighted  $I_{xx}$  and  $I_{yy}$  across the three taxa for the molar, premolar and symphyseal sections. We hence cannot definitively conclude that diet does have an effect.

On using the weighted moments of inertia compared to the unweighted moments, we found up to a 20% difference in values, and the difference was not predictable, hence not easily correctable if using the unweighted moments. We also found that the rank ordering within a sample group changes on using the weighted moments. All these findings seem to suggest that using weighted moments provides a more accurate and reliable method of comparing different cross sections. Our comparative tool incorporates both geometry and material distribution; hence we feel that this is a better method of comparison compared to the techniques and other indices used in the past in anthropology which relied exclusively on differences in geometry.

## APPENDIX A SAMPLE MATLAB CODES

Previously, a software program in Matlab™ had been developed by Dan Zahrly. The program was essentially a binary code. i.e. it made use of binary images (not grayscale) to get an answer. In that code, any grayscale image was converted into a binary image, read as 0 or 1, where 0 is black and 1 is white.

The program hence referred to the ‘shape’ and size of the image, and not the distribution of the grayscale within the image itself. As a consequence, the ‘real’ mechanical property of the bone section could not be ascertained, due to this significant loss of data. We thus wanted to find a way in which the ‘weight’ of each individual pixel could be accounted for, on a grayscale value (from 0 to 255- 0 being complete black and 255 being complete white).

The ‘Tooth removal’ Matlab code is given below. This code allows the user to remove the tooth and cancellous portion of bone from the rest of the section. The image is then directly saved in the selected folder, for further image analysis.

```
%- N.B.Bhatavadekar--%
clear all;
%---allows the user to pick the desired image for use with calculations
[filename, pathname]=uigetfile('*.bmp','Locate required datafile');
if(isempty(filename)|isempty(pathname))
    msgbox('Error on opening file!','READ FILE ERROR','error');
else
    A= imread(filename);
end
colormap gray
imshow(A)
```

```

A = double(A);
mask1 = double(roipoly);
mask2 = double(roipoly);
mask1 = -1.*(mask1 -1);
mask2 = -1.*(mask2 -1);
%%Apply Mask and convert image back to UINT8 format
newImage = A.*mask1.*mask2;
newImage = uint8(newImage);
imshow(newImage);
%%Set final Image
E = newImage;
figure, imshow(E); %---shows the image with the two deleted polygons

%-----Asks the user if they wish to add to the image
%button = questdlg('Do you want to add to the image?');
%if strcmp(button,'Yes')
% G2 = roipoly;
% G3 = double(G2)+E; %---adds the polygon to the image
%bw3 = im2bw(G3,0.5);
%figure, imshow(bw3); %---shows the altered image
%elseif strcmp(button,'No')
% bw3 = E;
% disp('Finishing Processing')

%elseif strcmp(button,'Cancel');
disp('Finishing Processing');
%end

%----Allows the user to delete additional sections of the image
%button = questdlg('You may now perform a final section of additional image
processing?');
%if strcmp(button,'Yes')
% J = roipoly; %----Allows the user to delet parts of the image
% J2 = roipoly; %----Allows the user to delet parts of the image
% bw4 = ~bw3; %--inverts the image so that "roipoly" will delete from the image
%K=double(J)+double(bw4)+double(J2); %---adds the incverted orginal image and
the selected (black) polygons
% L = ~K %---inverts the images so that it is "correct"
%figure, imshow(L); %---shows the image with the deleted sections

%-----Asks the user if they wish to add to the image
%button = questdlg('Do you want to add to the image?');
%if strcmp(button,'Yes')
% K2 = roipoly;
% K3 = double(K2)+L; %---adds the polygon to the image

```

```

% bw5 = im2bw(K3,0.5);
%figure, imshow(bw5); %---shows the altered image
%elseif strcmp(button,'No')
% disp('Finishing Processing')
%elseif strcmp(button,'Cancel');
% disp('Finishing Processing');
%end
%elseif strcmp(button,'No')
disp('Finishing Processing')
%elseif strcmp(button,'Cancel');
disp('Finishing Processing');
%end
%---reminder for the user to save the altered image
helpdlg('Remember to save this image (using the pull down menu) as a
BITMAP(xxx.bmp) for future use.');
```

%Save File

```

newImage = double(newImage);
imwrite((newImage/max(max(newImage))), 'filename.bmp', 'bmp');
```

The 'Image transform' code is given below. This code transforms the background of the images into a background with a grayscale value of zero, while maintaining the grayscale within the image cross-section.

```

clear; %---allows the user to pick the desired image for use with calculations
[filename, pathname]=uigetfile('*.bmp','Locate required datafile');
if(isempty(filename)|isempty(pathname))
    msgbox('Error on opening file!','READ FILE ERROR','error');
else
    I= imread(filename);
end
BWs = edge(I, 'sobel', (graythresh(I) * .1));

se90 = strel('line', 3, 90);
se0 = strel('line', 3, 0);

BWsdil = imdilate(BWs, [se90 se0]);
BWdfill = imfill(BWsdil, 'holes');
BWnobord = imclearborder(BWdfill, 4);

seD = strel('diamond',1);
BWfinal = imerode(BWdfill,seD);
BWfinal = imerode(BWfinal,seD);

Ifinal = uint8(double(I).*double(BWfinal));
```

```

imshow(Ifinal);
%Save File
newImage = double(Ifinal);
imwrite((newImage/max(max(newImage))), 'transform.bmp', 'bmp' );

```

The 'Weighted moment of inertia' Matlab code is represented below. An image file is selected, and the grayscale value of each pixel is used for the calculation of the moment of inertia.

```

clear; %---allows the user to pick the desired image for use with calculations
[filename, pathname]=uigetfile('*.*bmp','Locate required datafile');
if(isempty(filename)|isempty(pathname))
    msgbox('Error on opening file!','READ FILE ERROR','error');
else
    A= imread(filename);
end

%-----
prompt = {'Enter # of pixels/mm:'}; %---gets size of the specified BMP
title = 'Size of selected BMP';
lines= 1;
def = {'2.04'};
Y = inputdlg(prompt,title,lines,def);
Z = Y{1,1};
pix_mm = sscanf(Z,'%i');

%-----
image(A);%---First set of calculations-----
axis on;
imshow(A);
bw = A
figure, imshow(bw);
axis on;
bwarea(bw);
[r1,c1] = find(bw);
r = [r1]; %y values
c = [c1]; %x values
y2 = [r].*[r]; %y values squared
x2 = [c].*[c]; %x values squared
xy2 = [c].*[r]; %x/y vlaues squared

parea = ones(size(r)); %area of the dA's (pixels assumed to be one)

```

```

n = length(r);
for i=1:n
parea(i) = A(r(i),c(i));
end
Ixx1 = [y2].*[parea];
Ixx2 = sum(Ixx1);
Ixx = Ixx2/(pix_mm^4); %Ixx value

Iyy1 = [x2].*[parea];
Iyy2 = sum(Iyy1);
Iyy = Iyy2/(pix_mm^4); %Iyy value

Ixy1 = [xy2].*[parea];
Ixy2 = sum(Ixy1);
Ixy = Ixy2/(pix_mm^4); %Ixy value

Ixx = 0;
Iyy = 0;
Ixy = 0;

xbar1 = (sum([c].*[parea]))/(sum([parea]));
xbar = xbar1/pix_mm %xbar clac
ybar1 = (sum([r].*[parea]))/(sum([parea]));
ybar = ybar1/pix_mm %xbar clac
Ixxc1 = Ixx2-((ybar1)^2*(sum([parea])));
Ixxc = [Ixxc1/(pix_mm^4)]/255; %centrodial x moment clac
Iyyc1 = Iyy2-((xbar1)^2*(sum([parea])));
Iyyc = [Iyyc1/(pix_mm^4)]/255; %centrodial y moment clac
Ixyc1 = Ixy2-((ybar1)*(xbar1)*(sum([parea])));
Ixyc = [Ixyc1/(pix_mm^4)]/255; %centrodial xy moment clac
Ixxp1 = ((Ixxc1+Iyyc1)/2)+(((Ixxc1-Iyyc1)/2)^2+(Ixyc1)^2)^.5;
Ixxp = [Ixxp1/(pix_mm^4)]/255; %principal x moment calc
Iyyp1 = ((Ixxc1+Iyyc1)/2)-(((Ixxc1-Iyyc1)/2)^2+(Ixyc1)^2)^.5;
Iyyp = [Iyyp1/(pix_mm^4)]/255; %principal y moment calc
Ixyp = 0; %principal xy moment calc
thetaP = .5*atan((2*Ixyc1)/(Ixxc1-Iyyc1)); %orientation (thetaP) of the principal axes
wrt the centrodial axes

% Allows the user to enter a new axis, and then parallel axis theorem is used for
calculation of the new moment of inertia. This particular prompt was kept as an option,
but was in fact, never used during the analysis of any of the images
%.-----
%---User enters the location of the new axis-----
prompt = {'Enter the distance (mm) the new X axis is from the upper left hand corner:',
'Enter the distance (mm) the new Y axis is from the upper left hand corner:'

```

```

    'Enter the angular difference (in degrees) between the original axes and the new axes:'
};
title = 'New axes for calculations';
lines= 1;
def = {'0','0','0'};
S = inputdlg(prompt,title,lines,def);
P = S{1,1};
Q = S{2,1};
R = S(3,1);
C = char(R);
axisx = sscanf(P,'%i');
axisy = sscanf(Q,'%i');
T = sscanf(C,'%i')

%-----
%---New axis calculations (parallel axis theorem)---
Ixx_new2 = Ixxc1+((axisy)^2*(sum([parea])));
Ixx_new1 = Ixx_new2/(pix_mm^4); %new origin x moment clac
Iyy_new2 = Iyyc1+((axisx)^2*(sum([parea])));
Iyy_new1 = Iyy_new2/(pix_mm^4); %new origin y moment clac
Ixy_new2 = Ixyc1+((axisy)*(axisx)*(sum([parea])));
Ixy_new1 = Ixy_new2/(pix_mm^4); %new origin xy moment clac
theta = T/(180/pi);
Ixx_new = ((.5*(Ixx_new2+Iyy_new2))+(.5*(Ixx_new2- Iyy_new2)*cos(2*theta))-
(Ixy_new2*sin(2*theta)))/(pix_mm^4);
Iyy_new = ((.5*(Ixx_new2+Iyy_new2))-(.5*(Ixx_new2-
Iyy_new2)*cos(2*theta))+Ixy_new2*sin(2*theta))/(pix_mm^4);
Ixy_new = ((.5*(Ixx_new2-
Iyy_new2))*(sin(2*theta))+Ixy_new2*cos(2*theta))/(pix_mm^4);

%-----
%---changes the axes to the new axes on the displayed picture
axisx2 = axisx*pix_mm; %orientation of new x-axis in # of pixels
axisy2 = axisy*pix_mm; %orientation of new x-axis in # of pixels
u = (-((size(bw,2))-axisx2)*tan(theta))+axisy2; %unknown distance clacs. based on T
v = (((size(bw,1))-axisy2)*tan(theta))+axisx2; %unknown distance clacs. based on T
n2 = [axisx2 v]; %starting and end points of user-inputed axes
o2 = [axisy2 (size(bw,1))]; %starting and end points of user-inputed axes
p2 = [axisx2 size(bw,2)]; %starting and end points of user-inputed axes
q2 = [axisy2 u]; %starting and end points of user-inputed axes

%-----
%-----displaying the all axes-----
j = [xbar1 xbar1]; %starting and end points of centroidal axes
k = [ybar1 size(bw,1)]; %starting and end points of centroidal axes
l = [xbar1 size(bw,2)]; %starting and end points of centroidal axes

```

```

m = [ybar1 ybar1]; %starting and end points of centroidal axes
e = (-((size(bw,2))-xbar1)*tan(thetaP))+(ybar1); %unknown distance clacs. based on
thetaP
f = (((size(bw,1))-ybar1)*tan(thetaP))+(xbar1); %unknown distance clacs. based on
thetaP
n = [xbar1 f]; %starting and end points of principal axes
o = [ybar1 (size(bw,1))]; %starting and end points of principal axes
p = [xbar1 size(bw,2)]; %starting and end points of principal axes
q = [ybar1 e]; %starting and end points of principal axes

figure(1);
imagesc(bw); colormap(gray);
axis image;

hold on;
plot(j,k,'linewidth',2,'color', 'blue');
plot(n,o,'linewidth',2,'color', 'red');
plot(n2,o2,'linewidth',2,'color', 'yellow');
h = legend('Centroid','Principle Axes','User Specified Axes',3);
plot(1,m,'linewidth',2,'color', 'blue');
plot(p,q,'linewidth',2,'color', 'red');
plot(p2,q2,'linewidth',2,'color', 'yellow');
hold off;
%-----Display Theta-----
disp(['Theta: ',num2str(thetaP*180/pi)]);
%-----Display Ixx,Iyy,Ixc,Iyc,Ixp,Iyp-----
disp(['Ixx: ',num2str(Ixx)]);
disp(['Iyy: ',num2str(Iyy)]);
disp(['Ixc: ',num2str(Ixc)]);
disp(['Iyc: ',num2str(Iyc)]);
disp(['Ixp: ',num2str(Ixp)]);
disp(['Iyp: ',num2str(Iyp)]);
%----Saving stuff-----
f=fopen('Moment_Data.txt','wt');
fprintf(f,'\nMoment Calculations about the Axes Orginating in the Upper Left Corner\n');
fprintf(f,'Ixx = %g mm^4\n',Ixx);
fprintf(f,'Iyy = %g mm^4\n',Iyy);
fprintf(f,'Ixc = %g mm^4\n',Ixc);
fprintf(f,'Iyc = %g mm^4\n',Iyc);
fprintf(f,'Ixxc = %g mm^4\n',Ixxc);
fprintf(f,'Iyyc = %g mm^4\n',Iyyc);
fprintf(f,'Ixcy = %g mm^4\n',Ixcy);
fprintf(f,'Iycx = %g mm^4\n',Iycx);
fprintf(f,'Ixyp = %g mm^4\n',Ixyp);
fprintf(f,'Iyxp = %g mm^4\n',Iyxp);
fprintf(f,'Xbar = %g mm\n',xbar);
fprintf(f,'Ybar = %g mm\n',ybar);
fprintf(f,'ThetaP=%g rad\n',thetaP);

```

```

fprintf(f,'\nMoment Calculations about the User Specified Axes\n');
fprintf(f,'Ixx_new = %g mm^4\n',Ixx_new);
fprintf(f,'Iyy_new = %g mm^4\n',Iyy_new);
fprintf(f,'Ixy_new = %g mm^4\n',Ixy_new);
fclose(f);

```

The weighted moment of inertia program can be modified such that the grayscale power can be changed. The modification of this program is given below.

```

clear all; %---allows the user to pick the desired image for use with calculations
[filename, pathname]=uigetfile('*.*bmp','Locate required datafile');
if(isempty(filename)|isempty(pathname))
    msgbox('Error on opening file!','READ FILE ERROR','error');
else
    A= imread(filename);
end

%-----
prompt = {'Enter # of pixels/mm:'}; %---gets size of the specified BMP
title = 'Size of selected BMP';
lines= 1;
def = {'2.04'};
Y = inputdlg(prompt,title,lines,def);
Z = Y{1,1};
pix_mm = sscanf(Z,'%i');

% prompt2=('enter the power of grayscale: ');
% index=inputdlg(prompt2);
% ind=index{1,1};

ind=input('input grayscale power: ');

%-----
image(A);%---First set of calculations-----
axis on;
imshow(A);
bw = A;%bw = im2bw(A,0.5);
figure, imshow(bw);
axis on;
bwarea(bw);
[r1,c1] = find(bw);
r = [r1]; %y values
c = [c1]; %x values

```

```

y2 = [r].*[r]; %y values squared
x2 = [c].*[c]; %x values squared
xy2 = [c].*[r]; %x/y vlaues squared

n = length(r);
parea = ones(size(r)); %area of the dA's (pixels assumed to be one)
for i=1:length(r)
    pparea(i) = A(r(i),c(i));
end
pparea=double(pparea);
for i=1:n
    parea(i)=pparea(i).^ind;
end
% Ixx1 = [y2].*[parea];
Ixx1 = [y2].*[parea];
Ixx2 = sum(Ixx1);
Ixx = Ixx2/(pix_mm^4); %Ixx value

% Iyy1 = [x2].*[parea];
Iyy1 = [x2].*[parea];
Iyy2 = sum(Iyy1);
Iyy = Iyy2/(pix_mm^4); %Iyy value

% Ixy1 = [xy2].*[parea];
Ixy1 = [xy2].*[parea];
Ixy2 = sum(Ixy1);
Ixy = Ixy2/(pix_mm^4); %Ixy value

Ixx = 0;
Iyy = 0;
Ixy = 0;

xbar1 = (sum([c].*[parea]))/(sum([parea]));
xbar = xbar1/pix_mm %xbar clacs
ybar1 = (sum([r].*[parea]))/(sum([parea]));
ybar = ybar1/pix_mm %xbar clacs
Ixxc1 = Ixx2-((ybar1)^2*(sum([parea])));
Ixxc = [Ixxc1/(pix_mm^4)]/255; %centrodial x moment clac
Iyyc1 = Iyy2-((xbar1)^2*(sum([parea])));
Iyyc = [Iyyc1/(pix_mm^4)]/255; %centrodial y moment clac
Ixyc1 = Ixy2-((ybar1)*(xbar1)*(sum([parea])));
Ixyc = [Ixyc1/(pix_mm^4)]/255; %centrodial xy moment clac
Ixxp1 = ((Ixxc1+Iyyc1)/2)+(((Ixxc1-Iyyc1)/2)^2+(Ixyc1)^2)^.5;
Ixxp = [Ixxp1/(pix_mm^4)]/255; %principal x moment calc
Iyyyp1 = ((Ixxc1+Iyyc1)/2)-(((Ixxc1-Iyyc1)/2)^2+(Ixyc1)^2)^.5;
Iyyyp = [Iyyyp1/(pix_mm^4)]/255; %principal y moment calc

```

```

Iryp = 0; %principal xy moment calc
thetaP = .5*atan((2*Ixyc1)/(Ixxc1-Iyyc1)); %orientation (thetaP) of the principal axes
wrt the centroidal axes

%-----
%---User enters the location of the new axis-----
prompt = {'Enter the distance (mm) the new X axis is from the upper left hand corner:',
          'Enter the distance (mm) the new Y axis is from the upper left hand corner:',
          'Enter the angular difference (in degrees) between the original axes and the new axes:'
};
title = 'New axes for calculations';
lines= 1;
def = {'0','0','0'};
S = inputdlg(prompt,title,lines,def);
P = S{1,1};
Q = S{2,1};
R = S(3,1);
C = char(R);
axisx = sscanf(P,'%i');
axisy = sscanf(Q,'%i');
T = sscanf(C,'%i')

%-----
%---New axis calculations (parallel axis theorem)----
Ixx_new2 = Ixxc1+((axisy)^2*(sum([parea])));
Ixx_new1 = Ixx_new2/(pix_mm^4); %new origin x moment clac
Iyy_new2 = Iyyc1+((axisx)^2*(sum([parea])));
Iyy_new1 = Iyy_new2/(pix_mm^4); %new origin y moment clac
Ixy_new2 = Ixyc1+((axisy)*(axisx)*(sum([parea])));
Ixy_new1 = Ixy_new2/(pix_mm^4); %new origin xy moment clac
theta = T/(180/pi);
Ixx_new = ((.5*(Ixx_new2+Iyy_new2))+(.5*(Ixx_new2- Iyy_new2)*cos(2*theta))-
(Ixy_new2*sin(2*theta)))/(pix_mm^4);
Iyy_new = ((.5*(Ixx_new2+Iyy_new2))-(.5*(Ixx_new2-
Iyy_new2)*cos(2*theta))+Ixy_new2*sin(2*theta))/(pix_mm^4);
Ixy_new = ((.5*(Ixx_new2-
Iyy_new2))*(sin(2*theta))+Ixy_new2*cos(2*theta))/(pix_mm^4);

%-----
%---changes the axes to the new axes on the displayed picture
axisx2 = axisx*pix_mm; %orientation of new x-axis in # of pixels
axisy2 = axisy*pix_mm; %orientation of new x-axis in # of pixels
u = (-((size(bw,2))-axisx2)*tan(theta))+axisy2; %unknown distance clacs. based on T
v = (((size(bw,1))-axisy2)*tan(theta))+axisx2; %unknown distance clacs. based on T
n2 = [axisx2 v]; %starting and end points of user-inputed axes
o2 = [axisy2 (size(bw,1))]; %starting and end points of user-inputed axes

```

```

p2 = [axisx2 size(bw,2)]; %starting and end points of user-inputed axes
q2 = [axisy2 u]; %starting and end points of user-inputed axes

%-----
%-----displaying the all axes-----
j = [xbar1 xbar1]; %starting and end points of centroidal axes
k = [ybar1 size(bw,1)]; %starting and end points of centroidal axes
l = [xbar1 size(bw,2)]; %starting and end points of centroidal axes
m = [ybar1 ybar1]; %starting and end points of centroidal axes
e = (-((size(bw,2))-xbar1)*tan(thetaP))+(ybar1); %unknown distance clacs. based on
thetaP
f = (((size(bw,1))-ybar1)*tan(thetaP))+(xbar1); %unknown distance clacs. based on
thetaP
n = [xbar1 f]; %starting and end points of principal axes
o = [ybar1 (size(bw,1))]; %starting and end points of principal axes
p = [xbar1 size(bw,2)]; %starting and end points of principal axes
q = [ybar1 e]; %starting and end points of principal axes

figure(1);
imagesc(bw); colormap(gray);
axis image;

hold on;
plot(j,k,'linewidth',2,'color', 'blue');
plot(n,o,'linewidth',2,'color', 'red');
plot(n2,o2,'linewidth',2,'color', 'yellow');
h = legend('Centroid','Principle Axes','User Specified Axes',3);
plot(l,m,'linewidth',2,'color', 'blue');
plot(p,q,'linewidth',2,'color', 'red');
plot(p2,q2,'linewidth',2,'color', 'yellow');
hold off;
%-----Display Theta-----
disp(['Theta: ',num2str(thetaP*180/pi)]);
%-----Display Ixxc,Iyyc,Ixyc,Ixyp,Iyyp-----
disp(['Ixxc: ',num2str(Ixxc)]);
disp(['Iyyc: ',num2str(Iyyc)]);
disp(['Ixyc: ',num2str(Ixyc)]);
disp(['Ixyp: ',num2str(Ixyp)]);
disp(['Iyyp: ',num2str(Iyyp)]);
%---Saving stuff-----
f=fopen('Moment_Data.txt','wt');
fprintf(f,'\nMoment Calculations about the Axes Orginating in the Upper Left Corner\n');
fprintf(f,'Ixx = %g mm^4\n',Ixx);
fprintf(f,'Iyy = %g mm^4\n',Iyy);
fprintf(f,'Ixy = %g mm^4\n',Ixy);
fprintf(f,'Ixxc = %g mm^4\n',Ixxc);

```

```

fprintf(f,'Iyyc = %g mm^4\n',Iyyc);
fprintf(f,'Ixyc = %g mm^4\n',Ixyc);
fprintf(f,'Ixxp = %g mm^4\n',Ixxp);
fprintf(f,'Iyyp = %g mm^4\n',Iyyp);
fprintf(f,'Ixyp = %g mm^4\n',Ixyp);
fprintf(f,'Xbar = %g mm\n',xbar);
fprintf(f,'Ybar = %g mm\n',ybar);
fprintf(f,'ThetaP=%g rad\n',thetaP);
fprintf(f,'\nMoment Calculations about the User Specified Axes\n');
fprintf(f,'Ixx_new = %g mm^4\n',Ixx_new);
fprintf(f,'Iyy_new = %g mm^4\n',Iyy_new);
fprintf(f,'Ixy_new = %g mm^4\n',Ixy_new);
fclose(f);

```

The Matlab code developed by Dan Zharly is given below. I have referred to this code as the “Unweighted moment of inertia” code, as it is essentially a binary code i.e. it considers the pixels as having a grayscale value of either 0 (black) or 1 (white). A lot of information about the grayscale variation is hence lost.

```

%---Dan Zharly---%
clear; %---allows the user to pick the desired image for use with calculations
[filename, pathname]=uigetfile('*.bmp','Locate required datafile');
if(isempty(filename)|isempty(pathname))
    msgbox('Error on opening file!','READ FILE ERROR','error');
else
    A= imread(filename);
end

%-----
prompt = {'Enter # of pixels/mm:'}; %---gets size of the specified BMP
title = 'Size of selected BMP';
lines= 1;
def = {'3.9365'};
Y = inputdlg(prompt,title,lines,def);
Z = Y{1,1};
pix_mm = sscanf(Z,'%i');

%-----
image(A);%---First set of calculations-----
axis on;
imshow(A);
bw =A;
figure, imshow(bw);
axis on;
bwarea(bw);
[r1,c1] = find(bw);
r = [r1]; %y values

```

```

c = [c1]; %x values
y2 = [r].*[r]; %y values squared
x2 = [c].*[c]; %x values squared
xy2 = [c].*[r]; %x/y vlaues squared
parea = ones(size(r)); %area of the dA's (pixels assumed to be one)
Ixx1 = [y2].*[parea]
Ixx2 = sum(Ixx1);
Ixx = Ixx2/(pix_mm^4); %Ixx value
Iyy1 = [x2].*[parea];
Iyy2 = sum(Iyy1);
Iyy = Iyy2/(pix_mm^4); %Iyy value
Ixy1 = [xy2].*[parea];
Ixy2 = sum(Ixy1);
Ixy = Ixy2/(pix_mm^4); %Ixy value
xbar1 = (sum([c].*[parea]))/(sum([parea]));
xbar = xbar1/pix_mm %xbar clacs
ybar1 = (sum([r].*[parea]))/(sum([parea]));
ybar = ybar1/pix_mm %xbar clacs
Ixxc1 = Ixx2-((ybar1)^2*(sum([parea])));
Ixxc = Ixxc1/(pix_mm^4); %centrodial x moment clac
Iyyc1 = Iyy2-((xbar1)^2*(sum([parea])));
Iyyc = Iyyc1/(pix_mm^4); %centrodial y moment clac
Ixyc1 = Ixy2-((ybar1)*(xbar1)*(sum([parea])));
Ixyc = Ixyc1/(pix_mm^4); %centrodial xy moment clac
Ixxp1 = ((Ixxc1+Iyyc1)/2)+(((Ixxc1-Iyyc1)/2)^2+(Ixyc1)^2)^.5;
Ixxp = Ixxp1/(pix_mm^4); %principal x moment calc
Iyy1 = ((Ixxc1+Iyyc1)/2)-(((Ixxc1-Iyyc1)/2)^2+(Ixyc1)^2)^.5;
Iyy1 = Iyy1/(pix_mm^4); %principal y moment calc
Ixyp = 0; %principal xy moment calc
thetaP = .5*atan((2*Ixyc1)/(Ixxc1-Iyyc1)); %orientation (thetaP) of the principal axes
wrt the centrodial axes

%-----
%---User enters the location of the new axis-----
prompt = {'Enter the distance (mm) the new X axis is from the upper left hand corner:',
          'Enter the distance (mm) the new Y axis is from the upper left hand corner:',
          'Enter the angular difference (in degrees) between the orginal axes and the new axes:'
};
title = 'New axes for calculations';
lines= 1;
def = {'0','0','0'};
S = inputdlg(prompt,title,lines,def);
P = S{1,1};
Q = S{2,1};
R = S(3,1);
C = char(R);

```

```

axisx = sscanf(P,'%i');
axisy = sscanf(Q,'%i');
T = sscanf(C,'%i')

%-----
%---New axis calculations (parallel axis theorem)---
Ixx_new2 = Ixxc1+((axisy)^2*(sum([parea])));
Ixx_new1 = Ixx_new2/(pix_mm^4); %new orgin x moment clac
Iyy_new2 = Iyyc1+((axisx)^2*(sum([parea])));
Iyy_new1 = Iyy_new2/(pix_mm^4); %new orgin y moment clac
Ixy_new2 = Ixyc1+((axisy)*(axisx)*(sum([parea])));
Ixy_new1 = Ixy_new2/(pix_mm^4); %new orgin xy moment clac
theta = T/(180/pi);
Ixx_new = ((.5*(Ixx_new2+Iyy_new2))+(.5*(Ixx_new2- Iyy_new2)*cos(2*theta))-
(Ixy_new2*sin(2*theta)))/(pix_mm^4);
Iyy_new = ((.5*(Ixx_new2+Iyy_new2))-(.5*(Ixx_new2-
Iyy_new2)*cos(2*theta))+(Ixy_new2*sin(2*theta)))/(pix_mm^4);
Ixy_new = ((.5*(Ixx_new2-
Iyy_new2))*(sin(2*theta))+(Ixy_new2*cos(2*theta)))/(pix_mm^4);

%-----
%---changes the axes to the new axes on the diplayed picture
axisx2 = axisx*pix_mm; %orientation of new x-axis in # of pixels
axisy2 = axisy*pix_mm; %orientation of new x-axis in # of pixels
u = (-((size(bw,2))-axisx2)*tan(theta))+(axisy2); %unknown distance clacs. based on T
v = (((size(bw,1))-axisy2)*tan(theta))+(axisx2); %unknown distance clacs. based on T
n2 = [axisx2 v]; %starting and end points of user-inputed axes
o2 = [axisy2 (size(bw,1))]; %starting and end points of user-inputed axes
p2 = [axisx2 size(bw,2)]; %starting and end points of user-inputed axes
q2 = [axisy2 u]; %starting and end points of user-inputed axes

%-----
%-----displaying the all axes-----
j = [xbar1 xbar1]; %starting and end points of centroidal axes
k = [ybar1 size(bw,1)]; %starting and end points of centroidal axes
l = [xbar1 size(bw,2)]; %starting and end points of centroidal axes
m = [ybar1 ybar1]; %starting and end points of centroidal axes
e = (-((size(bw,2))-xbar1)*tan(thetaP))+(ybar1); %unknown distance clacs. based on
thetaP
f = (((size(bw,1))-ybar1)*tan(thetaP))+(xbar1); %unknown distance clacs. based on
thetaP
n = [xbar1 f]; %starting and end points of principal axes
o = [ybar1 (size(bw,1))]; %starting and end points of principal axes
p = [xbar1 size(bw,2)]; %starting and end points of principal axes
q = [ybar1 e]; %starting and end points of principal axes

```

```

figure(1);
imagesc(bw); colormap(gray);
axis image;

hold on;
plot(j,k,'linewidth',2,'color', 'blue');
plot(n,o,'linewidth',2,'color', 'red');
plot(n2,o2,'linewidth',2,'color', 'yellow');
h = legend('Centroid','Principle Axes','User Specified Axes',3);
plot(l,m,'linewidth',2,'color', 'blue');
plot(p,q,'linewidth',2,'color', 'red');
plot(p2,q2,'linewidth',2,'color', 'yellow');
hold off;
%-----Display Theta-----
disp(['thetaP: ',num2str(thetaP*180/pi)]);
%-----Display Ixxc,Iyyc,Ixyc,Ixxp,Iyyp-----
disp(['Ixxc: ',num2str(Ixxc)]);
disp(['Iyyc: ',num2str(Iyyc)]);
disp(['Ixyc: ',num2str(Ixyc)]);
disp(['Ixxp: ',num2str(Ixxp)]);
disp(['Iyyp: ',num2str(Iyyp)]);
%----Saving stuff-----
f=fopen('Moment_Data.txt','wt');
fprintf(f,'\nMoment Calculations about the Axes Originating in the Upper Left Corner\n');
fprintf(f,'Ixx = %g mm^4\n',Ixx);
fprintf(f,'Iyy = %g mm^4\n',Iyy);
fprintf(f,'Ixy = %g mm^4\n',Ixy);
fprintf(f,'Ixxc = %g mm^4\n',Ixxc);
fprintf(f,'Iyyc = %g mm^4\n',Iyyc);
fprintf(f,'Ixyc = %g mm^4\n',Ixyc);
fprintf(f,'Ixxp = %g mm^4\n',Ixxp);
fprintf(f,'Iyyp = %g mm^4\n',Iyyp);
fprintf(f,'Ixyp = %g mm^4\n',Ixyp);
fprintf(f,'Xbar = %g mm\n',xbar);
fprintf(f,'Ybar = %g mm\n',ybar);
fprintf(f,'ThetaP=%g rad\n',thetaP);
fprintf(f,'\nMoment Calculations about the User Specified Axes\n');
fprintf(f,'Ixx_new = %g mm^4\n',Ixx_new);
fprintf(f,'Iyy_new = %g mm^4\n',Iyy_new);
fprintf(f,'Ixy_new = %g mm^4\n',Ixy_new);
fclose(f);

```

## APPENDIX B VALIDATION OF MATLAB CODE

The figures were created using Microsoft Paint™. The images were opened as a file in Paintshop Pro7™, grayscaled using appropriate tools (from the Colors option in Paintshop Pro, select grayscale tool), saved as a file in Paintshop Pro, and then opened in the Matlab code. All images that were used were hence true grayscale images. The figures created were composite circles, rectangles and triangles.

Examples of such figures are below-

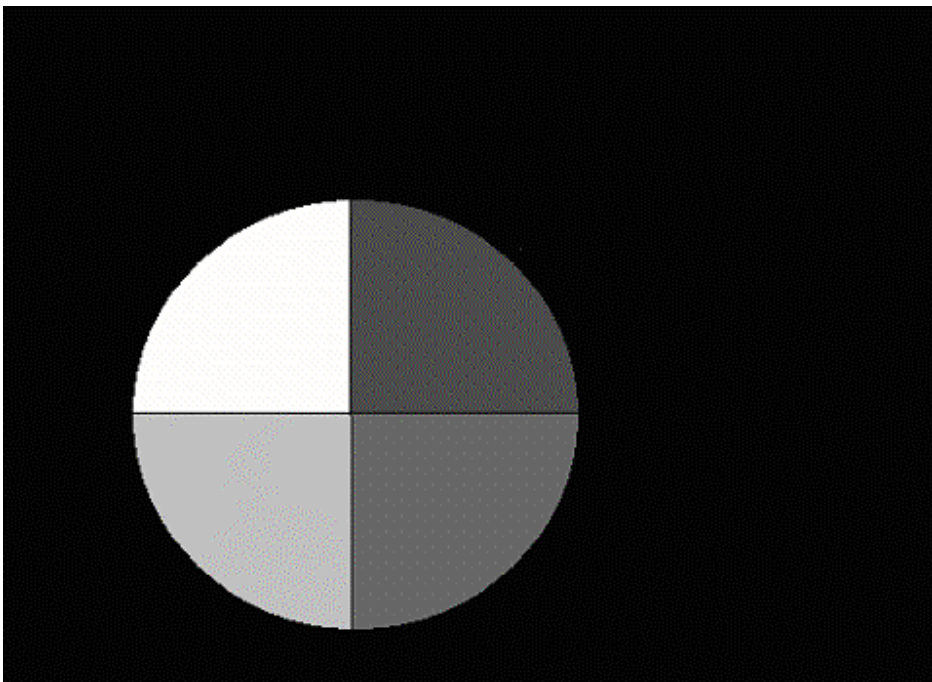


Figure B-1. Composite cross sectional figure with different grayscale values.

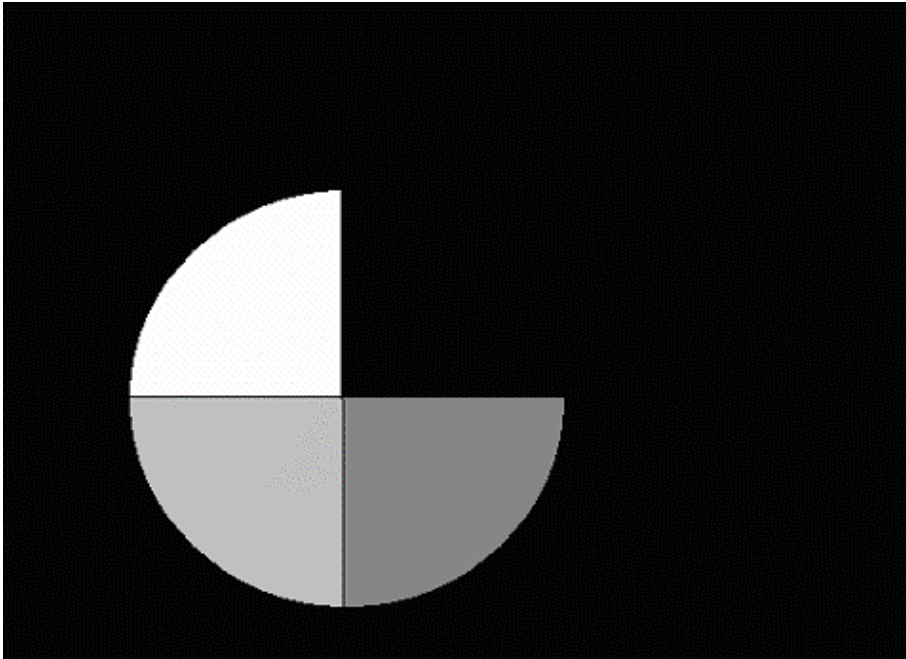


Figure B-2: Modification of Figure 1. The top right quadrant has been given the same grayscale value as the background (black-0).

As the dimensions of the figures, as well as the ‘weights’ were known, the centroids and angle between the new axes and the principal axes ( $\Theta$ ) were hand calculated for these figures. Each figure was then run through the newly developed Matlab code (henceforth referred to as ‘New Matlab code’). The program calculated the position of the centroid,  $I_{xx}$ ,  $I_{yy}$  (principal) and the new angle. ( $\Theta$ ).

The resultant positions of the centroid, and the angle, calculated by the ‘New Matlab code’ were as follows-

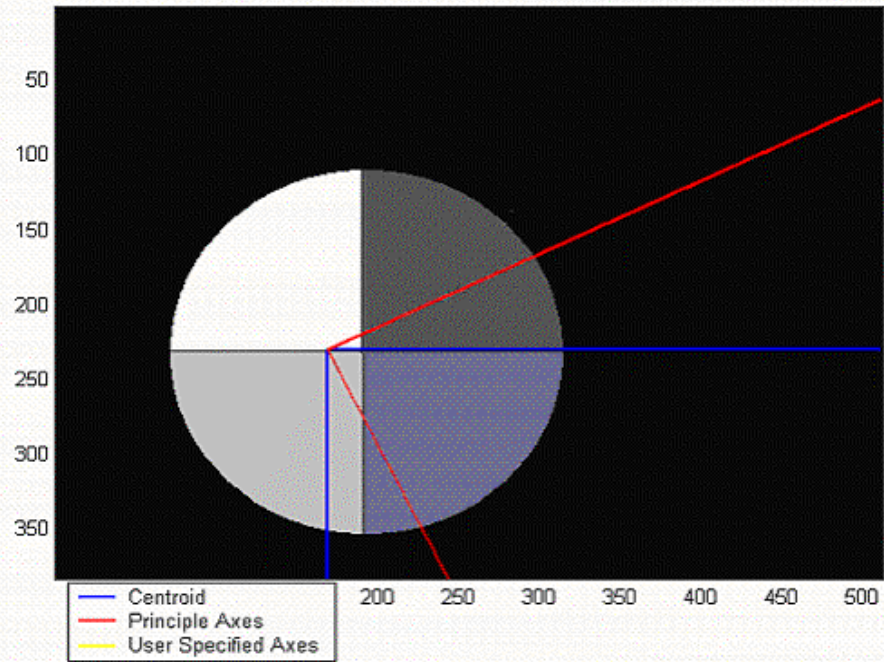


Figure B-3. Figure B-2 showing position of centroid and angle after running it through the New Matlab code.

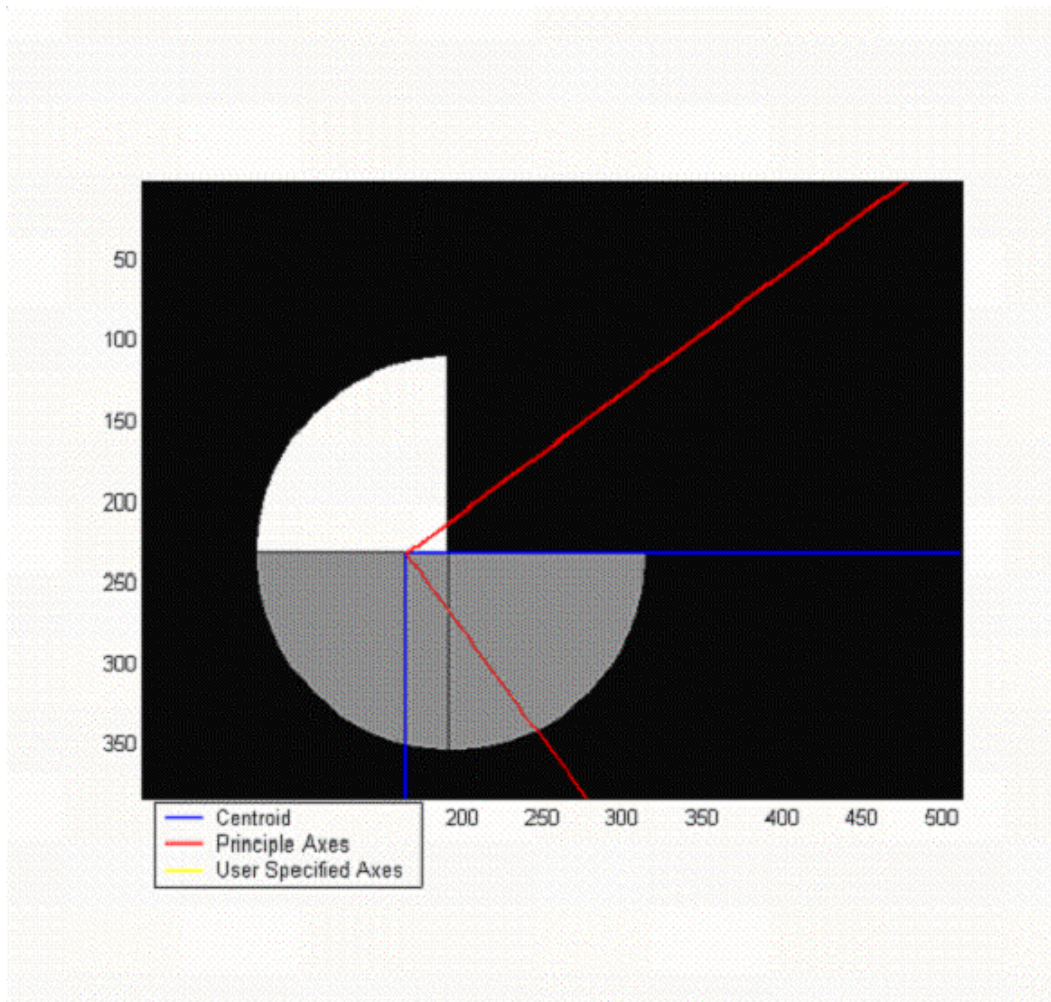


Figure B-4. Figure B-3 showing position of centroid and angle after running it through the New Matlab code.

The centroid was observed to shift down marginally in Fig.4, as compared to Fig.3. Also, the angle was seen to change by about 10 degrees, as was expected.

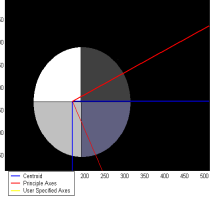
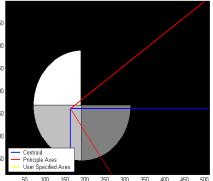
Figure	Hand-Calculated	Matlab Code
	Hand Calculated Centroid: ( 29.5,37.5)mm Theta: 31 degrees	Matlab code Centroid: ( 29.5,37.5)mm Theta: 31.07 degrees
	Hand Calculated Centroid: ( 28.1,36.1 ) mm Theta: 38 degrees	Matlab code Centroid: ( 28.2,36.2)mm Theta: 38.03 degrees

Figure B-5: Example of the comparison of results obtained for two composite circles with hand calculation and with the new Matlab code.

The hand-calculated results were compared with the results obtained through the New Matlab code. Both the results tallied for all figures, thereby validating the Matlab code.

## APPENDIX C IMAGE PROCESSING

Tomovision™ 1.2 Rev-14 software was used for opening the GE CT9800 images and converting them into 8-bit bitmap images. Each CT image had two sections- the right and left cross-section through the mandible. The section on the right side had been oriented correctly for the CT scan, hence this was the section to be considered. The section appearing on the left was a consequence of the scanner imaging it at an oblique angle, when scanning the right section. Hence, this section was an unwanted off spin of the imaging process on the right side, and this section was to be deleted in further processing of the CT image

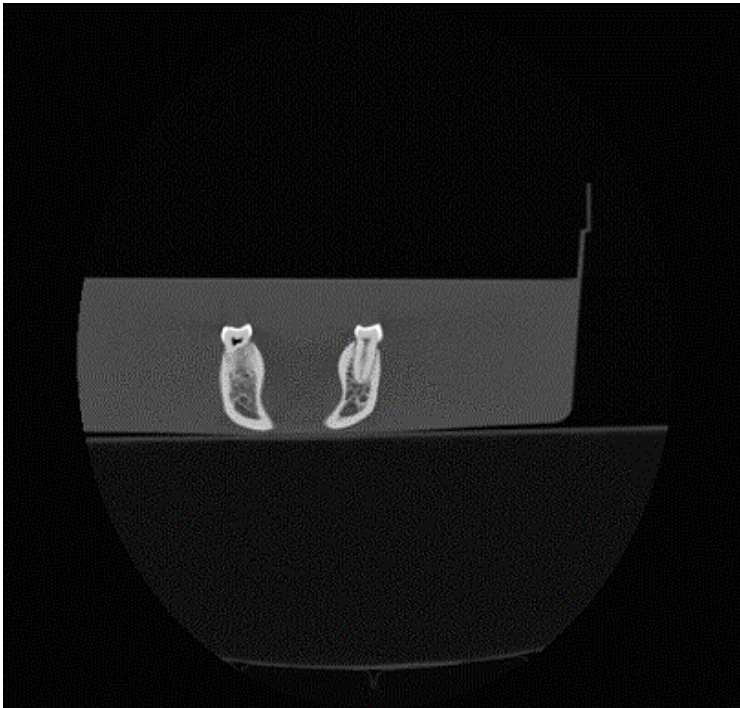


Figure C-1: CT image seen after converting it into a bitmap using Tomovision software. The section on the right is the one to be considered, while the one on the left is to be discarded. The sections can be seen placed in a water bath, when they were scanned.

After opening the image using Tomovision software, it is saved as a bitmap. Each image has two overlays – one showing the orientation of the image and the other displaying the parameters for the CT image. The parameters displayed are – 1)Image format 2)Image type 3) Table height 4) Scan time 5) Image position 6) Slice thickness 7) Pixel dimension 8)Tube voltage 9) Tube current. The overlays can be added on or removed from the image using the overlay tool in Tomovision. The image is then opened in Paintshop Pro, and cropped such that only the right section remains. (the image on the left is deleted).

The image is also cropped so as to crop away as much of the background as possible. (Since some of the images have been taken using a water bath, and some in air, the background for all images is not absolute black with grayscale value=0.If the background was left as is, then the background would also contribute some moment when the image was processed for biomechanical properties. Hence it is necessary to make sure that the background for all images is black, such that it doesn't contribute to the moment calculations in any way).By cropping away as much of the background as possible, we make it simpler to process the image with the subsequent Matlab image modification tool titled 'Image transform'.



Figure C-2: Image C-1 seen after cropping. The section seen is the right section, and the left has been deleted. (Image has been magnified here for clarity).

The image obtained has been cropped such that only the section to be considered for the biomechanical analysis is included, and the file is now in bitmap format (.bmp file extension). The bitmap format makes the image more versatile for use, in a variety of software programs, without a loss of the image information.

The tooth and cancellous bone can be removed by using the ‘Tooth Removal’ Matlab code. This code allows the user to remove the tooth and cancellous bone as two sections from the original image (by incorporating a ‘polygon’ removal function into the ‘Tooth removal’ program).

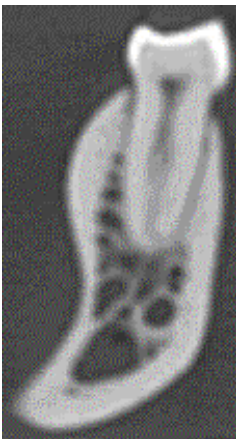


Figure C-3: Figure C-2 after background transformation using ‘Image transform’ Matlab code. (Image magnified here).

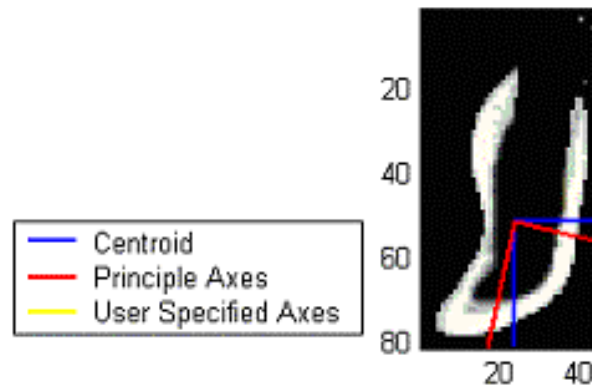


Figure C-4: Figure C-3 after running it through the ‘Weighted moment of inertia’ program. The user has the option of defining an axes parallel to the original axes. If this option is chosen, the ‘user specified axes’ will be displayed on the image. In the image above, these axes are not shown, as they were not selected.

The bitmap image is opened in Matlab version 6.5, and by running the ‘Weighted moment of inertia’ program. It is important to note that the file to be opened should be stored in the folder along with all other images to be sampled. This folder was named as ‘Jaw Moments’ folder. It also contained all the Matlab programs (e.g. for removal of tooth, image transformation, and background adjustment). The image files to be analyzed should not be stored in a sub-folder within the ‘Jaw Moments’ folder.

The Matlab program also gives the user the option of choosing a specified axis, at a certain distance from the x and y axes. The following shows an example of an output produced by the Matlab program after the analysis of an image-

Theta: -12.9147

I<sub>xxc</sub>: 2586.4431

I<sub>yyc</sub>: 806.1356

I<sub>xyc</sub>: -430.8799

I<sub>xxp</sub>: 2685.244

$I_{yyp}$ : 707.3348

The  $I_{xxp}$  ,  $I_{yyp}$  represent the moments of inertia along the principal axes respectively.  $\theta$  represents the angle that the new axes makes with respect to the orientation of the principal axes.

## APPENDIX D BASIC ANATOMY OF THE MANDIBLE

The chief anatomical landmarks in the human mandible are demonstrated in Figure 1. Apes have a similar gross mandibular anatomy, with a few modifications in the gonial angle, body and ramus.

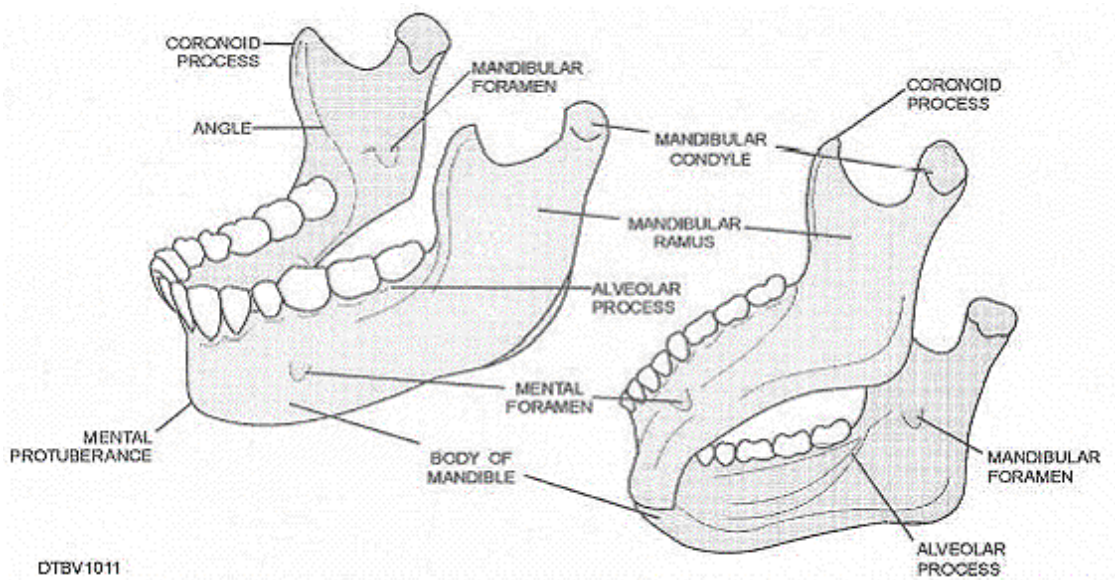


Figure D-1: Anatomical features in the human mandible.

[http://www.tpub.com/dental1/14274\\_files/image066.jpg](http://www.tpub.com/dental1/14274_files/image066.jpg), last accessed: 01/18/04.

The sections were taken from the molar, premolar and symphyseal regions. These three sections were best representative of the stress regions in the mandible.

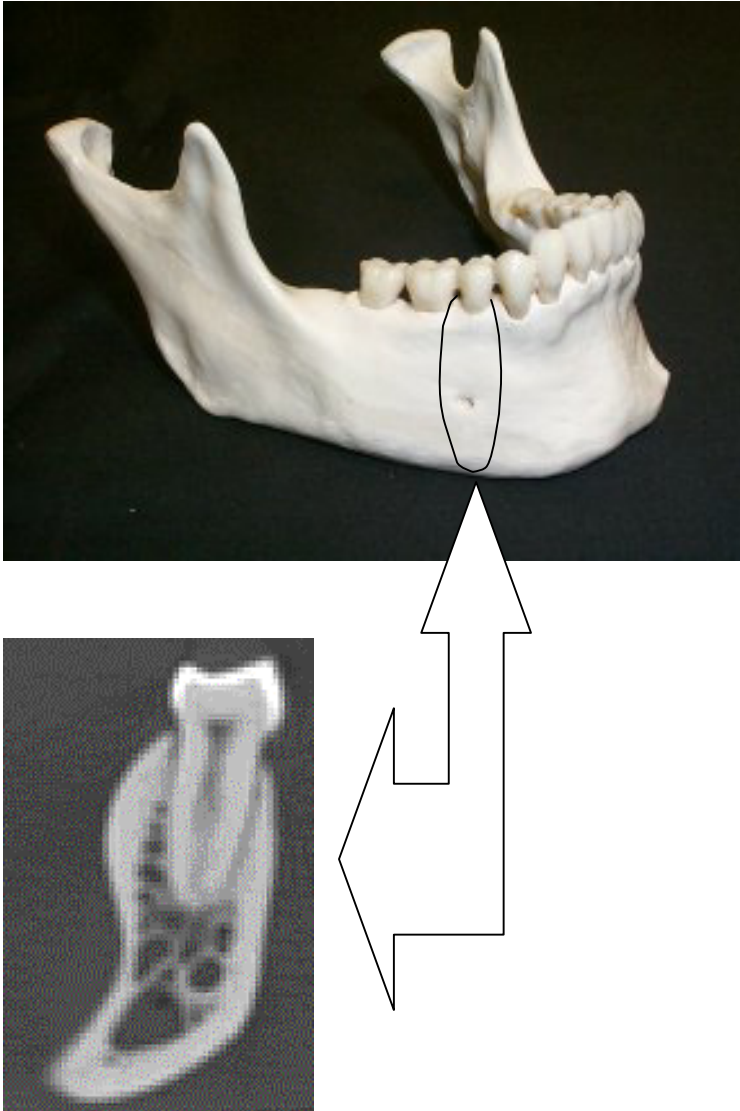


Figure D-2: Example of a CT scan taken through the premolar plane in the human mandible. For illustrative purposes, the mandible shown is a human mandible, while the cross section is actually a premolar section through an ape mandible. (Source: [a-s.clayton.edu/biology/BIOL1151L/lab05/skull\\_whole.htm](http://a-s.clayton.edu/biology/BIOL1151L/lab05/skull_whole.htm), last accessed: 01/24/04)

APPENDIX E  
ADDITIONAL RESULTS

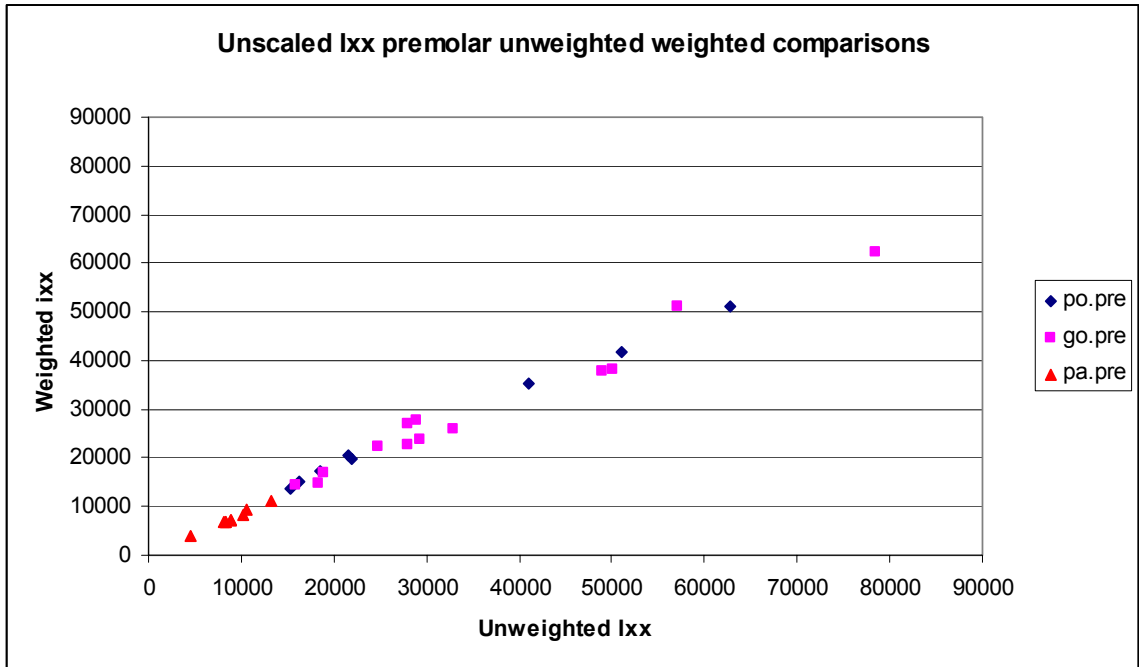


Figure E-1: Plot of premolar sections from Gorilla, Pongo and Pan. The unweighted Ixx values are after axes transformation to the weighted Ixx axes.

Figure 3-1 is a plot of the premolar sections of Gorilla, Pan and Pongo. The unweighted Ixx is the value for Ixx obtained after transforming the axes, to coincide with the weighted axes. We plotted this “raw” data (i.e. without scaling using appropriate parasagittal moment arms), as it would be a good reference point to compare the plots generated further, after scaling for jaw lengths. The values for Pan paniscus are seen to be the lowest amongst all the taxa for the plot in Figure E-1.

We compared two plots- 1) A plot of the unweighted Ixx versus the unweighted Ixx scaled for jaw length, with 2) A plot of the weighted Ixx versus the weighted Ixx scaled for jaw length. These plots are demonstrated in Figure E-2.

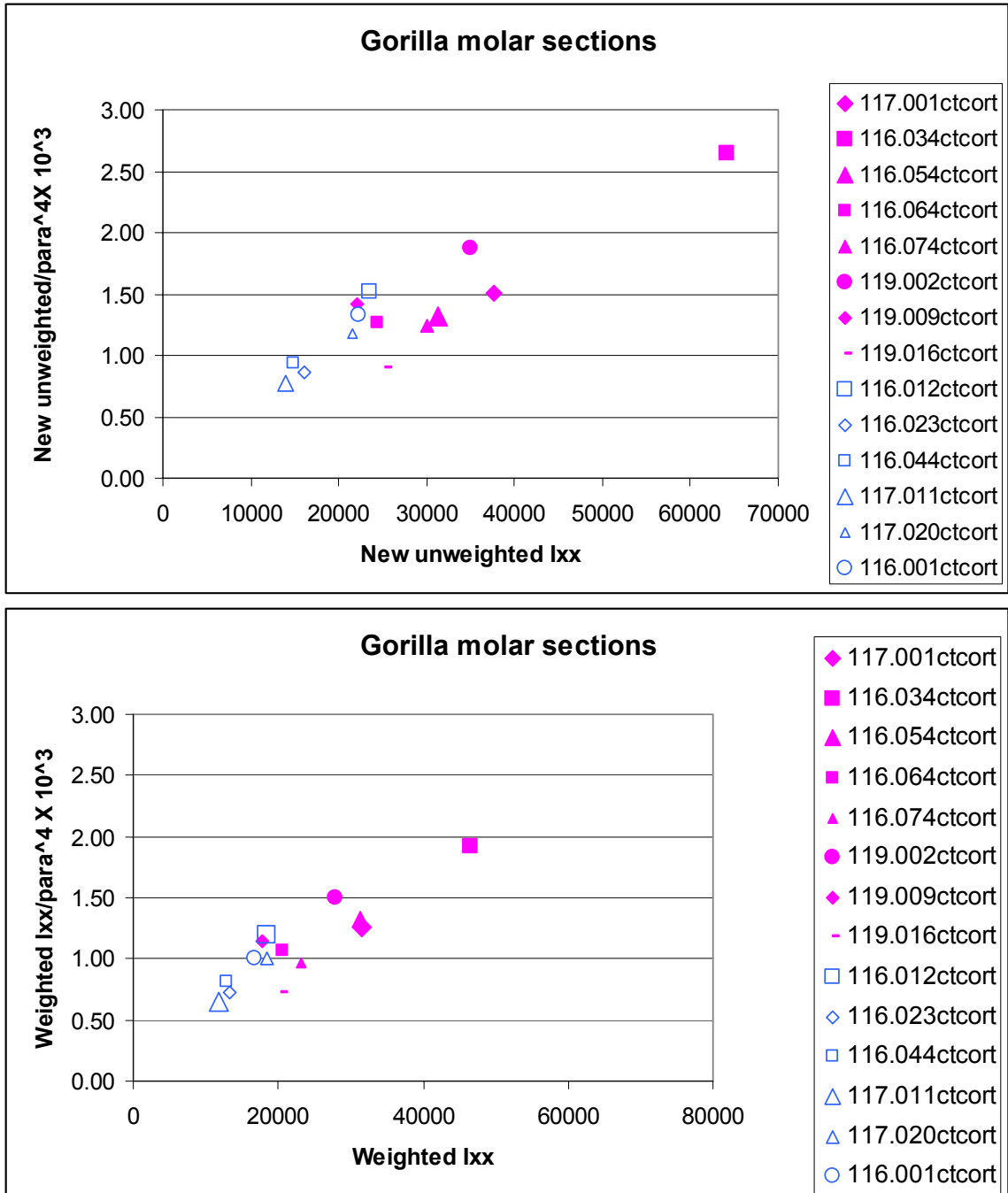


Figure E-2: Comparison of two plots of the Gorilla molar section demonstrating the change in rank ordering within the sample group before and after weighing the moments of inertia. In the legend, the filled symbols indicate male sections, while the open symbols indicate female sections.

We also plotted the unweighted versus the weighted Ixx and Iyy for all sections within the same taxon. The male and female sections were identified distinctly. Both the

weighted and unweighted  $I_{yy}$  were scaled appropriately for jaw length, using the wishboning moment arm length. Such a plot is demonstrated in Figure E-3 below. We observe that the values of the scaled  $I_{yy}$  are least for the symphyseal sections and the maximum for the molar sections.

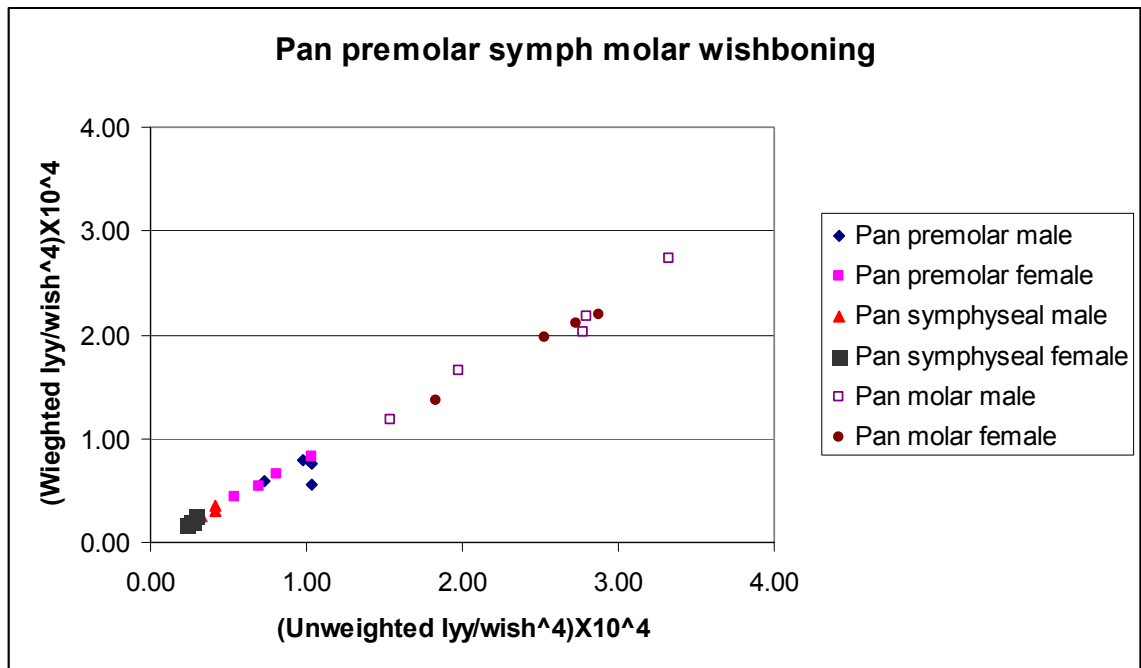


Figure E-3: Plot of the unweighted scaled  $I_{yy}$  versus the weighted scaled  $I_{yy}$  for the Pan symphyseal, premolar and molar sections.

### Effect of Grayscale power

When the grayscale power  $p$  is varied over two logarithmic decades, from 0.1 to 10, it is observed that the  $\theta_p$  increases very slightly. The results are shown in Figure E-4.

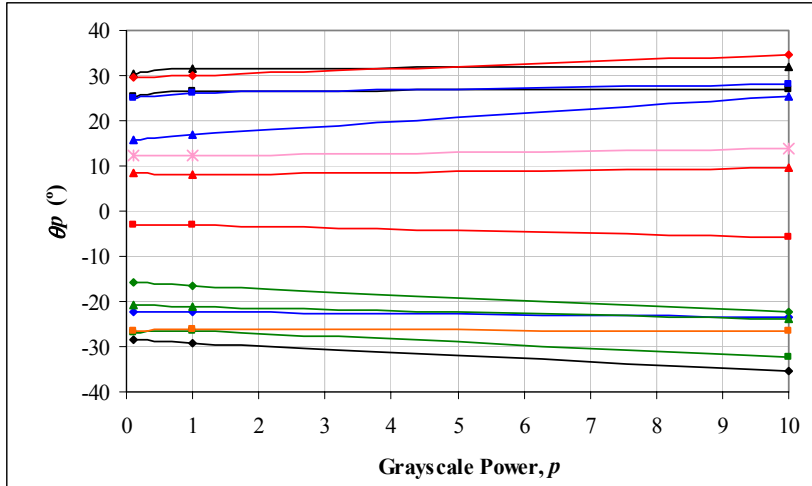


Figure E-4: Comparison of variation in theta ( $\Theta p$ ) with change in the  $p$ . Each gorilla molar section tested is represented by a different trend line.

## LIST OF REFERENCES

- Ciarelli TE, Fyhrie DP, Parfitt AM. 2003. Effects of vertebral bone fragility and bone formation rate on the mineralization levels of cancellous bone from white females. *Bone*. 2003 Mar; 32(3):311-5.
- Corcoran TA, Sandler RB, Myers ER, Lebowitz HH, Hayes WC. 1994. Calculation of cross-sectional geometry of bone from CT images with application in postmenopausal women. *J Comput Assist Tomogr*. 1994 Jul-Aug; 18(4):626-33
- Currey JD. 1988. The effect of porosity and mineral content on the young's modulus and elasticity of compact bone. *Journal of Biomechanics* 21 (1988), pp. 131-139
- Daegling DJ. 2001. Biomechanical scaling of the Hominoid Mandibular Symphysis. *J Morphology*. 250: 12-23
- Daegling DJ. 1992. Mandibular morphology and Diet in the Genus *Cebus*. *Int J Primatol*. Vol.13, No.5, 1992.
- Daegling DJ. 1989. Biomechanics of cross-sectional size and shape in the hominoid mandibular corpus. *Am J Phys Anthropol* 80: 91-106.
- Daegling DJ, Ravosa MJ, Johnson KR, Hylander WL. 1992. Influence of teeth, alveoli, and periodontal ligaments on torsional rigidity in human mandibles. *Am J Phy Anthropol* 89:59-72.
- Daegling DJ, Grine FE. 1991. Compact bone distribution and biomechanics of early hominid mandibles. *Am J Phys Anthropol*. 1991 Nov; 86(3):321-39.
- Demes B, Preuschoft H, Wolff JEA. 1984. Stress- strength relationships in the mandibles of hominoids. In: Chivers DJ, Wood BA, Bilsborough A, editors. *Food Acquisition and processing in primates*. New York: Plenum press. P. 369-390.
- Doran DM, McNeilage A, Greer D, Bocian C, Mehlman P, Shah N. 2002. Western lowland gorilla diet and resource availability: new evidence, cross-site comparisons, and reflections on indirect sampling methods. *Am J Primatol*. 2002 Nov; 58(3):91-116
- Fukunaga M, Tomomitsu T, Otsuka N, Imai H, Morita R, Nishii Y. 1990. Indexes of bone mineral content on second metacarpal bone roentgenogram analyzed by digital image processing: a comparison with other bone mass quantifying methods. *Radiat Med*. 1990 Nov-Dec; 8(6):230-5

- Gotzen N, Cross AR, Ifju PG, Rapoff AJ. 2003. Understanding stress concentration about a nutrient foramen. *J Biomech.* 2003 Oct; 36(10): 1511-21.
- Hounsfield, GN.1973. Computerized transverse axial scanning (tomography). I. Description of the system.*Br.J.Radiol.*46:1016-1022.
- Hylander WL.1979. Mandibular function in *Galago crassicaudatus* and *Macaca fascicularis*: an in vivo approach to stress analysis of the mandible. *J Morphol.* 1979 Feb; 159(2):253-96
- Hylander WL.1979.Mandibular function in *Galago crassicaudatus* and *Macaca fascicularis*: An in vivo approach to stress analysis of the mandible. *J Morphol.*159:253-296.
- Kuroda S.1992.Ecological interspecies relationships between gorillas and chimpanzees in the Ndoki-Nouabale Reserve,Northern Congo.In:Itiogawa N,Sugiyama Y,Sackett GP, Thomson RKR,editors.Topics in primatology.Vol II. Behavior, ecology and conservation. Tokyo: University of Tokyo.p 385-394.
- MacKinnon JR.1974.The behavior and ecology of wild orangutans (*Pongo pygmaeus*).*Anim Behav* 22:3-74.
- Mayhew.P, S.Kaptoge, N.Loveridge, J.Power, H.P.J.Kroger, M.Parker, and J.Reeve. 2004. Discrimination between cases of hip fracture and controls is improved by hip structural analysis compared to areal bone mineral density. An ex vivo study of the femoral neck. *Bone* 34(2004) 352-361.
- Nagurka ML, Hayes WC. 1980. An interactive graphics package for calculating cross-sectional properties of complex shapes.*J Biomechanics* 13:59-64.
- Ruff CB. The contribution of cancellous bone to long bone strength and rigidity. *Am J Phys Anthropol.* 1983 Jun; 61(2): 141-3.
- Ruff, CB, and Leo, FP.1986.Use of computed tomography in skeletal structural research.*Yrbk.Phys.Anthropol.*29:181-196.
- Schwartz GT.2000. Taxonomic and functional aspects of the patterning of enamel thickness distribution in extant large-bodied hominoids. *Am J Phys Anthropol.* ; 111(2): 221-44.
- Schwartz-Dabney CL and Dechow.PC.2003.Variations in cortical material properties throughout the human dentate mandible. *Am J Phys Anthropol* 2003.120:252-277.
- Taylor AB. Patterns of mandibular variation in Pan and Gorilla and implications for African ape taxonomy.
- Taylor AB. 2002.Masticatory form and function in the African Apes. *Am J Phys Anthropol* 117:133-156

- Tutin CEG, Ham R, White LJT, Harrison MJS. 1997. The primate community of the Lope reserve in Gabon; diet, responses to fruit scarcity, and effects on biomass. *Am J Phys Anthropol* 42:1-24.
- Ungar P. 1995. Fruit preferences of four sympatric primate species in Ketambe, northern Sumatra, Indonesia. *Int J Primatol* 16: 221-245.
- Weijs WA, de Jongh HJ. 1977. Strain in mandibular alveolar bone during mastication in the rabbit. *Arch Oral Biol.* 1977; 22(12):667-75
- Weiss S, Zimmerman MC, Harten RD, Alberta FG, Meunier A. 1998. The acoustic and structural properties of the human femur. *J Biomech Eng.* 1998 Feb; 120(1):71-6.

## BIOGRAPHICAL SKETCH

Neel Bhatavadekar completed his training in dentistry at the University of Bombay, India, with high honors. He was then selected as a trainee dental consultant at Bombay Hospital, concurrent with his selection as a research associate at the prestigious Indian Institute of Technology, Bombay.

While pursuing a master's degree in biomedical engineering at the University of Florida, he received a provisional patent for an invention dealing with a modification in skin harvesting technique for use in burns surgery. He is also the founding Vice-President of the Biomedical Engineering Graduate Student Association, and has received the Certificate of Academic Excellence from the UF International Center.

He plans to pursue a dental residency in periodontology upon graduation from UF.